

# 西安市第二十二届学术金秋激光红外学会分会 学术报告会暨2023年会员代表大会会议手册



西安市激光红外学会 主办  
陕西省计量科学研究院 共同主办

2023年9月23日

## 西安市激光红外学会简介

西安市激光红外学会（Xi'an Society of Laser and Infrared）成立于改革开放之初（1979 年春），是一个立足于西安市，由二十多家在激光、红外及光电科学领域有雄厚实力和国际声望的科研院所、高校和企业共同创建的学术性社会团体。学会常驻理事长单位为西北大学物理学院。目前拥有会员单位二十个左右，是一个方向性和学术性较强的社会团体。

学会的宗旨是为会员之间的学术和技术交流搭建平台，促进会员在激光、红外、光电领域的理论创新、技术创新、生产方式创新和产品创新，以提升会员的产学研交流水平，并最终以此为基础促进西安市、陕西省乃至我国在该领域的发展。

学会常年开展学术交流和技術交流活动。为充分发挥科技创新在创新发展中的引领作用，搭建高端、前沿、跨学科的学术交流平台，进一步提升学术交流质量，启迪创新思维、引领学科发展、培育创新人才，提高学会服务科技创新、服务西安率先创新发展的能力，学会每年组织开办西安市科协倡议的“学术金秋”活动，年均参会人数在二百余人。截至目前已经承办十九届“学术金秋”会议。

学会面向陕西省，甚至全国吸纳单位会员或个人会员，欢迎广大激光、红外和光电领域同仁入会交流。

西安市激光红外学会

二〇二三年九月

## 西安市第二十届学术金秋激光红外学会分会学术报告会暨西安市激光红外学会 2023 年会员代表大会议程

8:00-8:30	注册（主持人：学会副秘书长 <b>高爱华</b> 教授）
<b>8:30-8:35</b>	开幕式（主持人：学会理事长 <b>白晋涛</b> 教授）
8:35-8:50	民政局领导讲话
	市科协领导讲话
	计量科学研究院领导讲话 <b>周秉直</b> 正高工/院总工
<b>8:50-9:40</b>	西安市激光红外学会 2023 年会员代表大会暨第八届选举换届会议 （主持人：学会副理事长 <b>邵晓鹏</b> 教授）
8:50-8:55	奏唱《中华人民共和国国歌》
8:55-9:10	第七届工作报告：学会理事长 <b>白晋涛</b> 教授 第七届财务报告：学会副秘书长 <b>高爱华</b> 教授
9:10-9:20	宣读章程（草案）并表决
9:20-9:30	宣读第八届第一次会员代表大会选举办法
9:30-9:40	选举理事
<b>9:40-10:00</b>	合影/茶歇
<b>10:00-10:10</b>	西安市民政局社会组织管理局同志宣读理事会选举结果 并进行选举常务理事会和监事会

<b>10:10-12:10</b>	第一阶段学术报告 主持人: <b>巩稼民</b> 教授 (西安邮电大学)		
10:10-10:40	时间频率的测量及传递	<b>张首刚</b> 研究员	中国科学院国家授时中心
10:40-11:10	计算光学成像之范式探讨	<b>邵晓鹏</b> 教授	西安电子科技大学
11:10-11:40	激光跨尺度快速制造与超分辨成像监测技术研究进展	<b>王凯歌</b> 研究员	西北大学
11:40-11:55	陕西省计量科学研究院介绍	<b>周秉直</b> 正高工/院总工	陕西省计量科学研究院
11:55-12:10	硅基光子集成芯片光纤陀螺	<b>毛玉政</b> 高级工程师	航空 618 所
<b>12:10-12:15</b>	西安市民政局社会组织管理局同志宣读常务理事会和监事会选举结果		
<b>12:15-13:30</b> 午餐、参观			
<b>13:30-14:15</b>	第二阶段学术报告 主持人: <b>陈烽</b> 教授 (西安交通大学)		
13:30-13:45	LIBS 在线监控技术在激光清洗过程中的应用	<b>白杨</b> 教授	西北大学
13:45-14:00	时间门控激光拉曼光谱技术及应用	<b>张普</b> 研究员	中国科学院西安光学精密机械研究所
14:00-14:15	国家市场监管重点实验室(计量光学及应用)概况	<b>李奕</b> 正高工/国家市场监管 重点实验室主任	陕西省计量科学研究院

<b>14:15-15:15</b>	第三阶段学术报告 主持人:毛东 教授 (西北工业大学)		
14:15-14:30	基于精密色散补偿有源光纤环GHz 脉冲串飞秒激光技术研究	李峰 副研究员	中国科学院西安光学精密机械研究所
14:30-14:45	非球面制造过程中的高精度面形检测	李世杰 副教授	西安工业大学
14:45-15:00	基于 SPAD 阵列的激光雷达三维成像方法研究	康岩 助理研究员	中国科学院西安光学精密机械研究所
15:00-15:15	三维石墨烯制备与柔性传感应用	李连碧 教授李泽隆	西安工程大学
<b>15:15-15:25</b>	茶歇		
<b>15:25-15:55</b>	企业宣讲 主持人:王警卫 (西安炬光科技股份有限公司/首席科学家)		
15:25-15:30	西安炬光科技股份有限公司		
15:30-15:35	西安摘星光电科技有限公司		
15:35-15:40	霍克光仪(北京)科技有限公司		
15:40-15:45	长沙麓邦光电科技有限公司		
15:45-15:50	西安中科立德红外科技有限公司		
15:50-15:55	航空工业自控所		

<b>15:55-16:55</b>	第四阶段学术报告 主持人: <b>蔡长龙</b> 教授 (西安工业大学)		
15:55-16:05	金属碳化物 (NbC、TaC) 的宽带非线性特性及其应用	李二康 博士研究生	西北大学
16:05-16:15	Thickness-dependent terahertz emission from Bi <sub>2</sub> S <sub>3</sub> films under excitation below	席亚妍 博士研究生	西北大学
16:15-16:25	Interplay between Ultrafast Shift Current and Ultrafast Photon Drag Current in Tellurium Nanotubes	曹雪芹 博士研究生	西北大学
16:25-16:35	放电辅助激光诱导击穿光谱增强特性与应用研究	许博坪 硕士研究生	中国科学院西安光学精密机械研究所
16:35-16:45	辅助自由度下的四维 bell 态测量	范亚男 硕士研究生	西安工程大学
16:45-16:55	基于反射率修正的柱透镜面形光谱共焦测量研究	刘畅 硕士研究生	西安邮电大学
<b>16:55-17:45</b>	第五阶段学术报告 主持人: <b>李小军</b> 研究员 (西安空间无线电技术研究所)		
16:55-17:05	驻波场中手性粒子的散射及捕获特性	刘轩 硕士研究生	西安邮电大学
17:05-17:15	基于 LK 高斯金字塔的凸集投影距离像超分辨重构方法研究	周绪浪 硕士研究生	西安工业大学
17:15-17:25	一种基于铈酸锂环形开口结构的非线性超表面	孙越 硕士研究生	西安工程大学
17:25-17:35	具有纳米多孔GaN 分布布拉格反射镜的GaN 基发光器件的制备及特性研究	孙坤校 硕士研究生	西安工程大学
17:35-17:45	不同缀饰机制下的电磁感应吸收和透明	体浩伟 硕士研究生	西安工程大学

<p>17:45-18:00</p>	<p>优秀论文/优秀海报颁奖 一等奖：白晋涛 颁奖 二等奖：巩稼民 颁奖 三等奖：邵晓鹏 颁奖</p>
<p>18:00-18:10</p>	<p>闭幕式 (主持人：白晋涛 教授)</p>

# 学术海报展览

序号	张贴报告名称	姓名	工作单位
1	Self-sweeping regimes control in a bi-directional Yb-doped ring fiber laser	黄先明	西北大学
2	高维焦散光束的机理研究	管佳豪	西北大学
3	自聚焦光束的调控机理研究	何云东	西北大学
4	基于拓扑光子晶体环形谐振器的无源光学陀螺仪的理论研究	李港	西北大学
5	Topological states switching and group velocity control in two Dimensional non-reciprocal Hermitian photonic lattice	林宇	西北大学
6	拓扑光子晶体宽光谱慢光	彭晨阳	西北大学
7	铌酸锂波导中宽带二次谐波的产生	仝珍珠	西北大学
8	基于六芒星型的能谷光子晶体的拓扑边界态	万鑫	西北大学
9	迷宫寻宝光电智能小车	詹梓晨	西北大学
10	迷宫寻宝光电智能小车	曹依伦	西北大学
11	采用 DSMC 技术研究纳米孔中气体发射性质的研究	刘艳飞	西北大学
12	利用 RfS 技术研究 NpAA 双层纳米薄膜生长过程	王健飞	西北大学
13	使用深度神经网络实现荧光图像的超分辨转换	金子晨	西北大学



14	基于单分子成像技术研究 DNA 在微米通道中的运动特性	李志伟	西北大学
15	Non-iterative multifold strip segmentation phase method for six-dimensional optical field modulation	韩靓颖	西北大学
16	Study on the methods of fabricating glass devices based on 3D printing technology	佐方圆	西北大学
17	基于 GO-COOH 可饱和吸收体的 1 $\mu\text{m}$ 锁模光纤激光器	严义	西北大学
18	非互易厄米沙漏光子晶格能带调控及其光传输的影响	杨俊豪	西北大学
19	三格点胞内耦合控制的拓扑边界态	党煜	西北大学
20	Asymmetric Topological Edge States in One-Dimensional Trimer Lattices	张金	西北大学
21	Process development and monitoring in stripping of a C45E4 steel plate surface corrosion with 200 ns pulsed fiber laser	刘雪辰	西北大学
22	A high stability and low noise passively Q-switched yellow-green laser at 561 nm with a $\text{Ti}_3\text{C}_2\text{T}_x$ -PVA saturable absorber	王国珍	西北大学
23	Single-Longitudinal Mode Ytterbium-Doped Fiber Laser with Ultra-Narrow Linewidth and High OSNR Using a Double-Ring Passive Subcavity	文瀚	西北大学
24	激光参数对石材涂层脉冲激光清洗的影响	徐知微	西北大学
25	10kW 矩形光斑空间非相干合束器设计	闫佳乐	西北大学
26	Influence of laser parameters on corrosion resistance of laser melting layer on C45E4 steel surface	杨敬岩	西北大学
27	The mechanism of noise-like pulse in all-normal dispersion all-fiber laser based on nonlinear polarization rotation	郎嘉靖	西北大学

28	1.6- $\mu\text{m}$ Single-Frequency Erbium-doped Fiber laser based on a FP-FBG Filter and two cascaded Sub-Rings	翟雅琦	西北大学
29	基于 NALM 锁模的光纤激光器研究	杨雪育	西北大学
30	Passively Q-switched mode-locking Er-doped fiber laser with tunable wavelength and pulsating soliton	任陈旭	西北大学
31	All-PM Yb-doped mode-locked fiber laser with high single pulse energy and high repetition frequency	付超辉	西北大学
32	基于 NPR 的 C 波段和 L 波段锁模光纤激光器	王毅	西北大学
33	The interaction mechanism between Docetaxel and ctDNA based on the Laser Confocal Raman Spectroscopy	周苏丽	西北大学
34	In-situ construction of 2D/1D $\text{Bi}_2\text{O}_2\text{S}/\text{Bi}_2\text{S}_3$ heterojunction from the topotactic transformation of $\text{Bi}_2\text{O}_2\text{S}$ with significantly enhanced photoelectrochemical performance	张文静	西北大学
35	Defects regulation of $\text{Sb}_2(\text{S},\text{Se})_3$ by construction of $\text{Sb}_2(\text{S},\text{Se})_3/\text{CdSe}$ direct S-scheme heterojunction with enhanced photoelectrochemical performance	杨源灏	西北大学
36	The construction of $\text{Bi}_2\text{O}_2\text{S}/\text{ZnIn}_2\text{S}_4$ 2D heterojunction by cascade electric field with enhanced photoelectrochemical properties	魏雪玲	西北大学
37	Epitaxial growth strategy for construction of $\text{Tm}^{3+}$ doped and [hk1] oriented $\text{Sb}_2\text{S}_3$ nanorods S-scheme heterojunction with enhanced photoelectrochemical performance	刘鑫阳	西北大学
38	$\text{TiO}_2$ spatially confined growth of $\text{Sb}_2(\text{S},\text{Se})_3@/\text{TiO}_2$ NTs heterojunction photoanodes and their photoelectrochemical properties	金伟	西北大学
39	原位 Se 化构建 S 型 $\text{Sb}_2\text{S}_3@/\text{CdSe}_x\text{S}_{1-x}$ 核壳异质结及其光电化学特性	刘德康	西北大学
40	具有径轴向的 S 型 $\text{Sb}_2\text{S}_3/\text{In}_2\text{Se}_3$ 异质结光电极的构建及其光电化学性能的研究	马震	西北大学
41	$\text{Bi}_2\text{O}_2\text{S}$ topological transformation and in-situ regrowth of [hk1]-oriented $\text{SbBiS}_{3-x}\text{Se}_x$ 2D skeleton structure for construction of efficient quasi-two-dimensional $\text{Sb}_2\text{Se}_x\text{S}_{3-x}$ -based heterojunction photoanodes	张立媛	西北大学
42	大气压下氩气脉冲直流放电等离子体射流特性的数值模拟	高爱华、皇甫浩杰	西北大学

43	Manipulating nonlinear photocurrent from interlayer coupling in bilayer metamaterials for polarized terahertz generation	史明坚	西北大学
44	基于紫外光刻的光热型高耐久性液滴操控超滑表面	刘泽志	西北大学
45	Research and application advances of photo-responsive droplet manipulation functional surface	王新孔	西北大学
46	飞秒加工湿润功能表面与液滴操控研究	高文萍	西北大学
47	Techniques for Blood Cell Recognition and Behavior Tracking in Zebrafish	李紫钰	西北大学
48	基于svg路径解析和空间光调制器的多焦点并行加工技术	门飞燕	西北大学
49	激光高分子聚合物纳米制造技术及应用	刘一宁	西北大学
50	偏振光束通过圆柱形介质界面的紧聚焦研究	王怡洁	西北大学
51	Generation of Controllable Multi-focus Arrays Based on Phase Segmentation	杨玺萌	西北大学
52	基于 Nd/Yb 近红外双模光学温度传感探针的研究	李丹	西安邮电大学
53	一种基于泵浦调制技术的调 Q 锁模光纤激光器	陈雅妮	西安邮电大学
54	基于自适应遗传算法的自动锁模光纤激光器	郭若彤	西安邮电大学
55	基于 SSA-LSTM 方法的被动锁模光纤激光器脉冲特性沿腔内位置演化预测研究	张博媛	西安邮电大学

## 赞助企业海报展览

序号	张贴报告名称	赞助企业名称
1	北京茂丰光电科技有限公司企业宣介	北京茂丰光电科技有限公司
2	成都迈微信光电仪器有限公司企业宣介	成都迈微信光电仪器有限公司
3	西安摘星光电科技有限公司企业宣介	西安摘星光电科技有限公司
4	霍克光仪(北京)科技有限公司企业宣介	霍克光仪(北京)科技有限公司
5	深圳市麓邦技术有限公司企业宣介	深圳市麓邦技术有限公司

西安市第二十九届学术金秋会议激光红外学会  
分会学术报告会论文摘要集

西安市激光红外学会

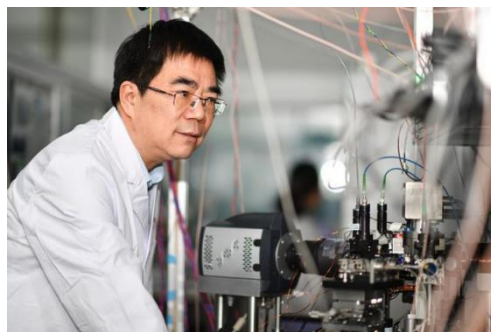
2023 年 9 月 23 日

# 时间频率的测量及传递

张首刚

中国科学院国家授时中心，西安 710600

在国际单位制的基本物理量中，时间是测量精度最高、应用最广的一个。本报告将介绍时间的概念及特征。围绕高精度时间频率的产生和传递，分别介绍不同类型的原子钟、时间频率测量仪器和天文时间测量手段的技术现状，以及时间频率精密传递方法和国家授时系统。此外，还将介绍我国空间站“高精度时间频率系统



“和国家重大科技基础设施“高精度地基授时系统”的主要目标和建设内容，以及时间频率研究的国内外差距。

张首刚，研究员，博士生导师，现任中国科学院国家授时中心主任，中国科学院时间频率基准重点实验室主任。历任中科院国家授时中心量子频标研究团组首席研究员、中科院国家授时中心主任助理、副主任。长期从事原子钟及其应用的研究。兼任国家自然科学基金重大研究计划“精密测量物理”指导专家组成员、SKA专项专家组成员、全国导航设备标准化技术委员会主任、中国天文学会时间专业委员会主任、国际天文学会时间工作组组长等。

# 计算光学成像之范式探讨

邵晓鹏

西安电子科技大学光电工程学院，西安 710071

作为下一代成像技术，计算光学成像通过引入信息技术，利用光场调制和解译实现传统成像的性能突破和边界扩展，极具发展潜力。计算成像的灵魂是光场，引擎是升维。如何构建光场，如何设计引擎，报告围绕计算光学成像的范式，探讨基于高维光场的计算成像模型。归纳分析高维光场的表征量以及高维光场到低维投影之间的信息传递映射关系，重点讨论如何有效且针对性地使用降维后光场信息实现性能突破的问题。作为信息获取终端的探测器，其设计及使用也应该遵循以光场的有效投影和信息传递最优为主要准则的范式要求，探索未来光电成像模型，改变光电成像的格局。



邵晓鹏，教授，西安电子科技大学光电工程学院院长，西安市计算成像重点实验室主任，173重点项目首席，科普作家。主要研究方向：计算光学成像技术、光电图像处理与模式识别、光电仪器研制与测试。现任国家部委专业组专家，中国光学工程学会常务理事、中国光学学会理事、陕西省光学学会副理事长、陕西省光学工程学会副理事长、西安市激光红外学会副理事长；光场调控及其系统集成应用福建省高校重点实验室学术委员会主任；国防工业光电信息控制和安全技术等 10 余个重点实验室学术委员会委员。《Advanced imaging》主编，《Ultrafast Science》副主编，《应用光学》副主任委员，《激光与光电子学进展》《光学精密工程》《光子学报》《系统工程与电子技术》《数据采集》《光电技术应用》《激光与红外》《集成技术》《西安电子科技大学学报》等期刊编委。

## 激光跨尺度快速制造与超分辨成像监测技术研究进展

王凯歌

西北大学光子学与光子技术研究所，西安 710127

目前，包括纳米尺寸单元为核心的功能结构及其器件的制备方法与技术，在信息科学、材料科学、生命科学、国防建设等领域得到了广泛关注和快速发展。具有纳米精度的制造受到光学衍射极限的限制、也难以在线检测，制造周期长、效率低；亟需发展同时具有纳米精度快速制造与无损在线监测功能的技术与方法。本报告简单介绍我们在研制跨尺度结构的超分辨光学快速制造系统过程中，为实现跨纳米-微米-毫米结构且尺度连续可调一体化制造、同时具有纳米精度原位测量等功能所开展的研究工作进展情况，主要包括多光束同轴共焦、多焦点非迭代阵列生成与调制、光束六维动态可调、矢量路径多焦点并行控制、单纳米尺寸制造等方面。



王凯歌，研究员/教授，博士生导师。陕西省“光电子与纳米光子技术生物医学应用创新团队”负责人；陕西省“科技创新领军人才”；陕西省“光电子技术重点实验室”主任；“国家级光电技术与纳米功能材料国际联合研究中心”副主任。陕西省光学学会副理事长；陕西省物理学会理事；中国光学学会生物医学光子学专委会常务委员；《光子学报》、《应用光学》编委；担任国家自然科学基金函评/会评专家、国家科学技术进步奖等函评专家；担任多个国际物理与纳米科技等领域期刊常期评审专家；多次担任国内外学术会议分会主席、学术委员会委员；发表专业学术SCI论文130余篇、授权专利12项等。

## LIBS 光谱监测用于材料表面除锈除漆

白杨

西北大学光子学与光子技术研究所, 西安 710127

by@nwu.edu.cn

**摘要:**介绍了在基于LIBS 方法和图像处理方法的协同使用, 分析不同激光参数(包括平均激光功率、光斑重叠比和清洗次数)对材料表面除锈除漆激光清洗效率和质量的影响规律, 研制出一套激光清洗在线监测系统。分别以 Q235B 低碳钢板锈蚀层、石质文物表面油漆层的激光清洗为实例展开, 结果表明, LIBS 光谱探测结合图像处理可以在有效保护材料表面的基础上, 确定最佳激光参数。LIBS 法对化学成分变化响应速度快, 能够对微小面积锈蚀层激光清洗实施在线监测, 但重复性差。图像处理法能够直观地对大面积锈蚀层实施激光清洗作业后的在线评估, 但灵敏度不高。LIBS 法与图像处理法协同使用, 能够避免各自缺陷, 达到对大面积激光清洗过程的自动化监控, 有助于确定最佳激光参数、提高激光清洗效率。

**关键字:**激光清洗, LIBS 光谱在线监测, 图像识别法, 过程监控

为了解决的大面积金属表面锈蚀层激光清洗过程的实时监测和控制(监控)问题, 搭建了一套基于图像处理法和 LIBS 分析法协同的激光清洗过程监控系统。以 Q235B 低碳钢板锈蚀层、石质文物表面油漆层的激光清洗为具体实例, 激光清洗过程监控是准确去除金属锈蚀层、有效避免金属基体损伤的关键。利用图像处理技术研究了较大面积 Q235B 钢板在不同光斑搭接率下的清洗次数与清洗度的变化规律, 得到最佳光斑搭接率。利用LIBS 光谱研究了微小面积 Q235B 钢板的皮尔逊相关系数随清洗次数的变化趋势, 得到了不同厚度锈蚀层下的最佳清洗次数。激光清洗后的钢板样品的锈蚀率仅为 40.86%, 防腐性能提升将近 50%, 激光清洗后的钢板样品具备了耐腐蚀能力。激光参数的选择不仅影响激光清洗过程中石质文物表面是否受损, 而且直接影响石质文物去除油漆层的质量和效率。LIBS光谱探测结合图像处理可以在有效保护石质文物表面的基础上, 确定最佳激光参数。利用图像法研究了激光清洗汉白玉表面金色、银色油漆的清洗度以及清洗速率变化趋势, 获取最佳激光光斑搭接率和最佳清洗次数。采用图像法对激光清洗汉白玉表面油漆层的清洗效果进行评估。95.1%的金漆激光清洗度和 97.2%银漆激光清洗度表明, LIBS 法和图像法的协同使用可有效提高汉白玉表面油漆层的激光清洗效率。

**English Title:** Interplay between Ultrafast Shift Current and Ultrafast Photon Drag Current in Tellurium Nanotubes

Xueqin Cao

Northwest University, Xi'an 710069, China

**Abstract:** Photocurrent induced by nonlinear optical effects has innovated fundamental optic physics in optoelectronic devices, including nonlinear photodetectors, nonlinear optical absorbers, and solar cells. The cooperative interaction between different kinds of nonlinear photocurrents would be a complex yet interesting issue. The THz wave of tellurium (Te) nanotube films is generated from the interplay between the ultrafast shift current and ultrafast photon drag current, which are ascribed to the photogalvanic effect (PGE) and photon drag effect (PDE), respectively. According to the THz emission spectroscopy excited from opposite incident planes, the contribution ratio of the PDE and PGE is calculated as 1.2:1 for the THz parallel EHz-p component and 1:1 for the perpendicular EHz-s component under the p-polarized excitation. The different ratios between these two components are related to the different nonlinear susceptibility tensor elements. These results highlight the THz emission spectroscopy as an effective tool to clarify the interplay mechanism between different nonlinear photocurrents.

**Key Words:** tellurium (Te) nanotubes, terahertz (THz) emission, photogalvanic effect (PGE), photon drag effect (PDE), shift current

**Text:**

Photocurrent induced by nonlinear optical effects have sparked interests for improving the performance of optoelectronic and photonic devices.<sup>[1-3]</sup> This so-called nonlinear photocurrent breaks is beneficial to minimize the energy loss,<sup>[4]</sup> thereby taking a crucial step towards high-efficiency photovoltaic devices. Previously, the nonlinear photocurrent response is measured via a *dc* electrical technique with external electrodes.<sup>[5,6]</sup> However, the electrode contact would cause parasitic interface effects to the photocurrent response.

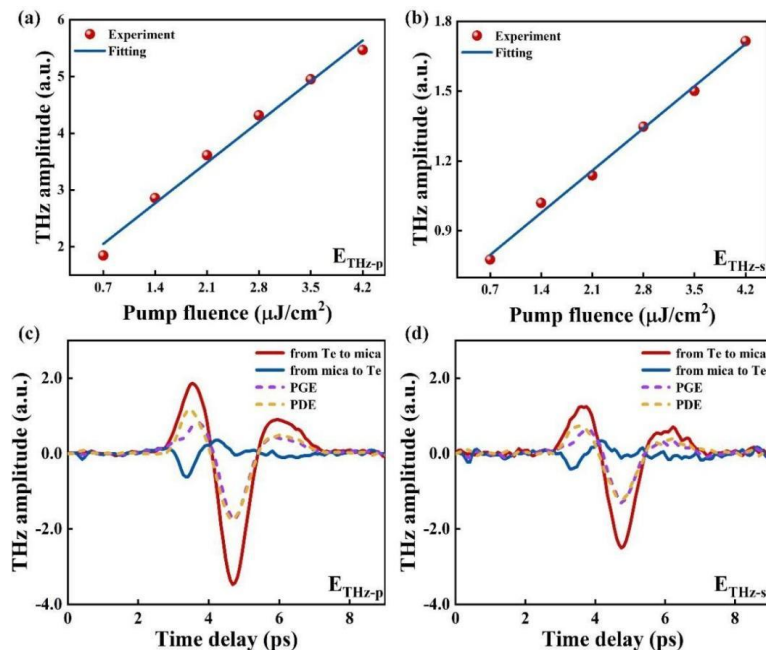


In this work, combined with the THz emission dependences on the pump fluence and the incident wave vector, the THz radiation mechanism of Te nanotube films is ascribed to the concurrent photogalvanic effect (PGE) and photon drag effect (PDE). This study could lay a foundation for the applications of the Te nanostructures in the next-generation optoelectronic devices.

With the pump fluence increasing from 0.7 to 4.2  $\mu\text{J}/\text{cm}^2$ , the THz amplitude increases linearly with the pump fluence, which are well fitted by the linear function as shown in Figure 1(a-b). This result validates the dominant mechanism based on the second-order nonlinear optical effects.<sup>[7]</sup> In Figure 1(c-d), changing the illumination direction from the Te side or from the mica side is equivalent to reversing the wave vector of the incident light. We can separate the THz emission signals generated from the PGE and PDE as shown in Figure 1(c-d). The results suggest that the contribution of the PDE to the THz radiation is 1.2 times larger than that of the PGE for the  $E_{\text{THz-p}}$  component, while the contribution ratio between the PDE and PGE is approximate 1:1 for the  $E_{\text{THz-s}}$  component.

In conclusion, the physical mechanisms the Te nanotubes are ascribed to the cooperative interaction of the ultrafast shift current and the ultrafast photon drag current. Besides, according to the incident wave vector dependence of the THz radiation, the contribution ratio of the PDE and PGE to the THz radiation is calculated as 1.2: 1 to the THz  $E_{\text{THz-p}}$  component and 1:1 for  $E_{\text{THz-s}}$  component.

This slight difference is caused by the different nonlinear susceptibility tensor elements.



This work deepens the understanding of the different photocurrent response between Te and its 1D nanostructures.

Figure 1. Pump fluence dependence of the THz amplitude for (a) the  $E_{\text{THz-p}}$  component and (b)  $E_{\text{THz-s}}$  component. The time-domain signals of (c) the  $E_{\text{THz-p}}$  component and (d)  $E_{\text{THz-s}}$  component excited from the Te side (red line) and from the mica side (blue line). The purple and yellow dashed lines represent the THz radiation from the single PGE and PDE, respectively.

References

- [1] Villanueva-Cab J, Wang H, Oskam G, et al. Electron diffusion and back Reaction in dye-sensitized solar cells: the effect of nonlinear recombination kinetics[J]. The Journal of Physical Chemistry Letters, 2010, 1(4): 748-751.
- [2] Ryzhii V, Ryzhii M, Svintsov D, et al. Nonlinear response of infrared photodetectors based on van der Waals heterostructures with graphene layers[J]. Optics Express, 2017, 25(5): 5536-5549.
- [3] Chang Y M, Kim H, Lee J H, et al. Multilayered graphene efficiently formed by mechanical exfoliation for nonlinear saturable absorbers in fiber mode-locked lasers[J]. Applied Physics Letters, 2010, 97(21): 211102.
- [4] Mu X, Pan Y, Zhou J. Pure bulk orbital and spin photocurrent in two-dimensional ferroelectric materials[J]. npj Computational Materials, 2021, 7(1): 61.

- [5] Khun K, Ibupoto Z H, Willander M. Development of fast and sensitive ultraviolet photodetector using p-type NiO/n-type TiO<sub>2</sub> heterostructures[J]. *Physica Status Solidi a-Applications and Materials Science*, 2013, 210(12): 2720-2724.
- [6] Saushin A S, Mikheev G M, Vanyukov V V, et al. The Surface Photogalvanic and Photon Drag Effects in Ag/Pd Metal-Semiconductor Nanocomposite[J]. *Nanomaterials (Basel)*, 2021, 11(11): 2827.
- [7] Huang Y, Zhu L, Zhao Q, et al. Surface optical rectification from layered MoS<sub>2</sub> crystal by THz time-domain surface emission spectroscopy[J]. *ACS Applied Materials & Interfaces*, 2017, 9(5): 4956-4965.

## Control of excitation light coupled to a single fluoride crystal with waveguide structure to enhance upconversion luminescence

*Qingyan Han\**, *Shixing Fan*, *Wei Gao*, *Yunxiang Li*, *Hao Zhang*, *Zihan Liu*, *Chengyun Zhang*, and *Jun Dong\**

School of Electronic Engineering, Xi'an University of Posts and Telecommunications, Xi'an 710121 China

\* E-mail: qyhan@xupt.edu.cn; dongjun@xupt.edu.cn

**Abstract:** Lanthanide (Ln)-doped upconversion luminescence (UCL) materials have aroused extensive scientific attention due to their remarkable and unique optical properties, such as excellent photostability, large anti-Stokes shift, deep excitation penetration, narrow emission bandwidth, and long lifetimes<sup>[1]</sup>. However, how to effectively improve their UCL efficiency has always been an important scientific issue. Here, we design and fabricate  $\beta$ -NaYF<sub>4</sub> microtubes (MTs) with a natural hexagonal shape in the cross section and wedge shape on both top vertexes, which can be regarded as an optical waveguide<sup>[2]</sup>. The UCL property of a single  $\beta$ -NaYF<sub>4</sub>:Yb<sup>3+</sup>/Er<sup>3+</sup>/Tm<sup>3+</sup> (or Tm<sup>3+</sup>) MT is systematically investigated based on waveguide-excitation modes. It is found that the excitation light can be efficiently coupled in the  $\beta$ -NaYF<sub>4</sub>:Yb<sup>3+</sup>/Er<sup>3+</sup> (or Tm<sup>3+</sup>) MT by modulating the angle between the wedge-shape end plane of MT and the microscope slide. In addition, it is clearly observed that the excitation light can be confined and propagate in the MT by introducing a 633 nm laser, which is mainly due to the natural waveguide structure with a stronger confinement and propagation effect of light, thereby enhancing light-to-MT interactions. The current work provides a powerful solution to build high-efficiency Ln-doped UCL materials, which may have potential applications in the optical communication and biomedical fields.

**Keywords:** near-infrared light; enhancement; nanocrystals; patterns; films

## 辅助自由度下的四维bell 态测量

范亚男

西安工程大学, 西安 710600

摘要: 贝尔态 (Bell-state) 测量在量子通信领域中有着十分重要的作用, 但如何实现完整的bell 态测量仍然没有一个明确的方案。本文提出了一个利用偏振自由度 (DOF) 和频率自由度作为辅助手段, 完成四维轨道角动量 (OAM)-bell 态测量的理论方案。在这个方案中, 我们先定义了由 OAM-偏振-频率这 3 个自由度纠缠的超纠缠态作为输入态, 再将输入态通过由量子逻辑门组成的超纠缠态分析仪, 由于量子逻辑门能对单个自由度响应, 那么输入的超纠缠态经过分析仪后将会转化为一个全新的态。通过理论计算我们可以得知 16 个输入态与 16 个输出态的对应关系, 根据单光子的投影测量结果, 能得到输出态的形式, 最终实现四维模式下的OAM-bell 态测量。同时, 此方案作为扩展量子通信容量的一个新途径, 对实现大容量量子通信有着重要意义。

关键词: 量子通信, bell 态测量, 辅助自由度, 超纠缠态

## SPAD 阵列激光雷达三维成像方法研究进展

康岩\*, 薛瑞凯, 李薇薇, 王晓芳, 梁锦涛, 李力飞, 张同意\*

中国科学院西安光学精密机械研究所瞬态光学与光子技术国家重点实验室, 西安 710119

kangyan@opt. ac. cn

摘要:基于单光子雪崩二极管 (SPAD) 探测器的激光雷达因具备高探测灵敏度和高时间分辨能力在远距离三维成像、自动驾驶及目标探测等领域受到广泛关注。然而,目前各像素带独立定时电路的SPAD 阵列探测器仍然存在像素规模小、填充率低及热像素噪声大等问题,这使得难以直接利用其实现高分辨率、高质量三维成像。为提升SPAD 阵列激光雷达三维成像性能,设计并搭建了一套基于衍射光学元件产生光束阵列与SPAD 阵列光敏面高精度配准的共轴单光子激光雷达三维成像系统,对 50 m~180 m 范围内不同目标进行了三维成像实验验证;提出了基于亚像素扫描和像素复用的三维成像方法,通过亚像素细分扫描提高了成像分辨率,同时通过像素复用克服了 SPAD 阵列的热像素影响;提出并开展了基于强度图像引导的利用小面阵SPAD 进行深度成像的研究,通过设计时空联合噪声滤除算法并利用融合目标强度信息的广义全变分正则化重建方法,以无扫描方式实现了成像横向分辨率  $4\times 4$  倍增强。

关键词:单光子计数, 激光雷达, 三维成像, 亚像素, SPAD 阵列

## 金属碳化物的宽带非线性特性及其应用

李二康

西北大学, 西安 710119

lierkang12@163. com

摘要:金属碳化物(NbC 和TaC),作为新兴的二维材料,具有优异的导电性、宽带线性光响应和强的光与物质相互作用。然而,NbC 和TaC 在光通信波段的非线性光学性质的未被探索,这极大地限制了宽带光子器件的发展。在此,我们用Z 扫描系统测量了NbC 和TaC 在近红外波段的无色散可饱和吸收。NbC 和TaC 表现出了优于石墨烯、NbC 和TaC 等金属材料的非线性吸收系数,这可以用三能级模型很好的解释。在近红外区域展现出来的可饱和吸收使NbC 和TaC 成功地应用到全光调制器中,实现了>40%的调制深度;并在调Q 激光器中实现了微秒级别的脉冲。这些结果表明了NbC 和TaC 在高性能光子器件的应用中有着巨大的潜力。

关键词:NbC&TaC, 宽带可饱和吸收, 金属碳化物, 全光调制器, 调Q 激光器

为了测量NbC 和TaC 的光学非线性吸收响应,我们搭建了具有宽波段、短脉冲(50 fs)光源的开口 Z 扫描系统。图(a)和(b)展示了NbC和TaC在1064-1700 nm 波段范围的可饱和吸收特性。由于NbC 和TaC的金属特性,价带电子很容易被激发到导带,进一步增加激发光的强度就会发生由泡利阻塞引起的光漂白现象,这就是可饱和吸收现象发生的本质。更详细、直观的描述如下。根据计算得出的能带结构中发现电子能带与费米能级处于交叉状态,利用这一性质可以判断 NbC 和TaC 属于金属材料。在高泵浦光激发下,光生热电子很容易从价带被激发到导带中。当被激发的电子数量足够多时,会填满导带中的空位。如果继续增加激发光的泵浦强度时,激发光不会被样品吸收,这就是可饱和吸收特性的直观表现。

基于NbC 和TaC 的可饱和吸收特性,我们利用 980 nm 的脉冲光(10 kHz)作为泵浦光区调制 1550 nm 的连续光(信号光)。当泵浦光增加到一定程度就会激发样品的可饱和吸收特性,此时泵浦光的载波信息就会加载到信号光中,如图 2(a-b)所示,这就意味着信号光被调制。为了评估调制器的性能,不同泵浦功率下的调制深度被计算,如图 2(c-d)所示,表现出来NbC 和 TaC 都具有>40%的调制深度,进而说明了调制器的高性能。

为了进一步证明NbC 和 TaC 在光子学器件中应用价值,将其放入光纤环形激光腔中调节腔的增益与损耗实现调Q 脉冲。图 3(a-b)描述了泵浦功率在 280 mW 和 260 mW 时,NbC 和TaC 激光器输出的重复频率为了 34.4 kHz 和 32.3 kHz 的脉冲序列。对应的单脉冲包络如图 3(c-d)所示,脉冲宽度分别为 3.04  $\mu$ s 和 2.9  $\mu$ s。此外,信噪比作为一个描述激光器稳定的重要参数,在频谱中可以体现出来。如图 3(e-f)所示, $\geq 70$  dB 的信噪比说明激光器的稳定性很高。最后,为了探测激光器的工作波长,光谱被测量,如图(g-h)所示,其工作波长分别为 1564.4 nm 和 1568.3 nm。

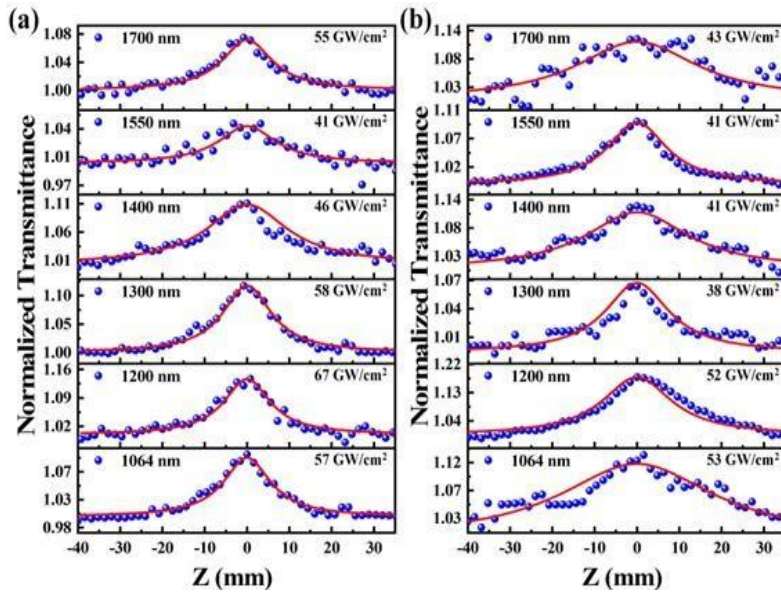


图1 (a) NbC 和 (b) TaC 的非线性光学响应。

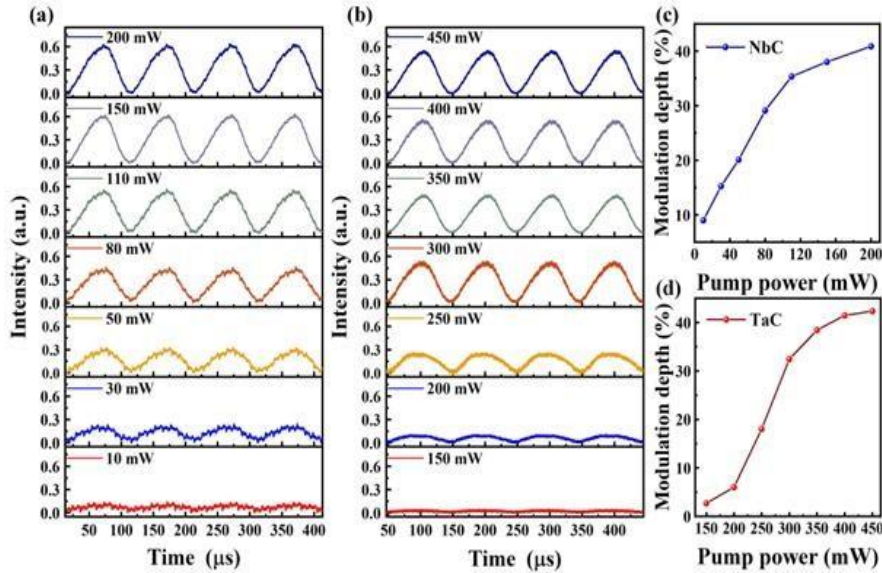


图2 基于(a) NbC 和 (b) TaC 的调制结果；在 (c) NbC 和 (d) TaC 调制器中，调制深度与泵浦功率的关系。

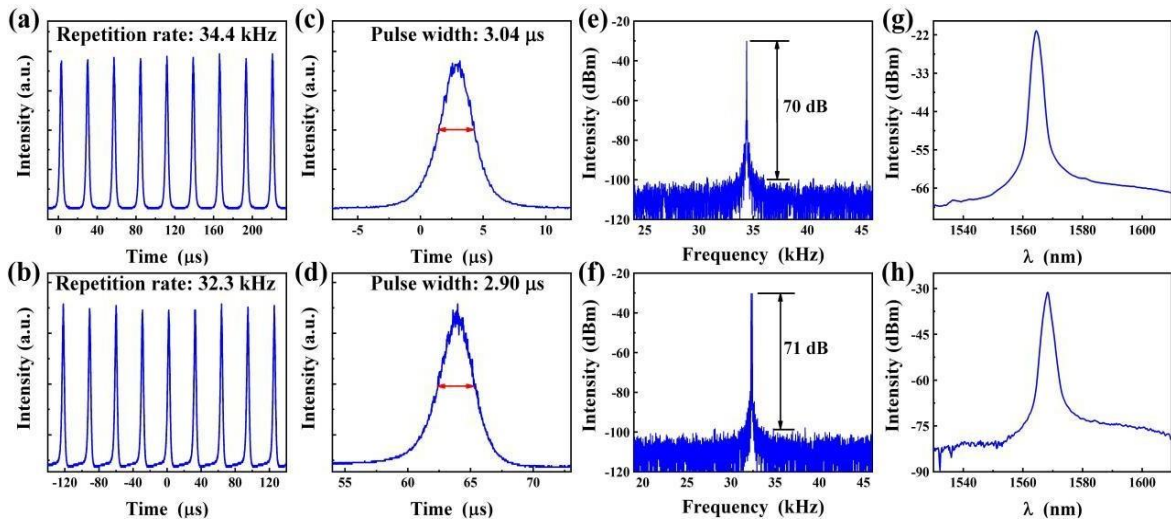


图3 NbC 和 TaC 调Q 激光器的 (a-b) 脉冲序列、(c-d) 单脉冲包络、(e-f) 频谱和 (g-h) 光谱。

## 基于精密色散补偿的有源光纤环 GHz 脉冲串飞秒激光技术研究

李峰\*、王屹山\*、李强龙、曹雪、温文龙、行纪欣

中国科学院西安光学精密机械研究所瞬态光学与光子技术国家重点实验室, 西安 710119

lifeng@opt.ac.cn; yshwang@opt.ac.cn

摘要:GHz 频率下的脉冲串激光器(Burst mode)目前在材料加工领域越来越受到关注,研究发现目前GHz 脉冲可以在材料去除效率上实现提升,但是如此高的重复频率的锁模脉冲产生目前还面临着较大的挑战,高重复频率要求极短的激光腔长,将导致光纤激光器的熔接制作和固体振荡器的集成化难题的出现。本研究采用自研的高稳定的 34.38 MHz 的半导体可饱和吸收镜(SESAM)全光纤锁模激光振荡器作为种子源,通过一个分数比为  $2 \times 2$  的耦合器,将光脉冲分为两束,一束直接输出,另外一束通过一个精密色散补偿的光纤环实现和另外一束的脉冲堆叠,实现 GHz 级别的高重复频率脉冲输出。在精密色散补偿的光纤环内,加入了声光开关实现脉冲串重复频率调控。光纤环输出后采用另外一个具有同步延时的声光调制器,实现对脉冲串输出个数的调控,实现 GHz 的 burst 脉冲串输出。同时,采用啁啾光纤光栅进行了脉冲的压缩,不同输出脉冲个数下的脉冲宽度测试都可以保证在 400–500 fs 之间,验证了光纤环实现了近零色散的精密色散补偿。本研究结果将为材料的高效飞秒激光加工探索一条新的技术途径。

## 三维石墨烯制备与柔性传感应用

李泽隆, 李连碧\*, 朱长军, 张国青, 李泽斌

西安工程大学理学院, 710048

xpu\_lilianbi@163.com

摘要:三维结构的石墨烯在避免二维石墨烯的堆叠的同时,保留了石墨烯的固有特性,表现出了二维石墨烯无法观察到的电学和光学现象,例如,孔隙结构,高表面活性以及与光的高相互面积等。基于这些优异的性能,三维石墨烯材料广泛应用于锂离子电池、光催化、3D GFET 光电探测器等领域。本文报告了可控高精度的三维石墨烯制备方法,使用等离子体刻蚀法,制备图形化的二维石墨烯,并使用光刻技术将其三维结构化。同时,创新性地以 Porous- $n\text{C}_{12}\text{H}_{12}\text{O}_{11}$  作为牺牲模板,制备了高弹性多孔结构的泡沫骨架,进一步制备了 3D 石墨烯/PDMS 复合材料。利用三维石墨烯材料制备了柔性传感器。该器件表现出优异的压敏特性,在 5V 偏压下,当外加压力从 0 增加到 1.92N 时,电导率增大 302%,对微压力的响应表现十分出色;由暗状态转变为辐照时(光功率密度为  $5.0 \text{ W/cm}^2$  的强光),该器件电导率增大了 55%,具有压敏/光敏双功能。同时,该器件还具有空间光角分辨能力,在传感器领域有很好的应用潜力。

关键词:三维石墨烯, 传感器, 光敏, 压敏

## 基于反射率修正的柱透镜面形光谱共焦测量研究

李春艳, 刘畅, 刘继红, 李丹琳, 蒋杰伟

(西安邮电大学 电子工程学院, 陕西 西安 710121)

L17829090670@163.com

摘要:为实现柱透镜面形的精确测量,对反射率引起的面形测量误差进行了研究。首先介绍了光谱共焦位移传感系统的工作原理,并在空间坐标系下利用柱透镜的结构参数,推导了系统的光谱响应,建立了柱透镜面形测量模型。然后,对各点反射率引起的光谱曲线谱峰漂移,进而造成的面形测量误差进行了理论研究及仿真分析,为修正透镜曲面反射率对测量结果的影响,提出采用 S-G 滤波及高斯拟合实现滤波和光谱信号峰值波长的提取,建立了反射率误差修正算法,最后通过搭建实验平台,完成了基于反射率修正的柱透镜面形测量。实验结果表明:修正前面形测量结果的平均绝对误差和均方根误差分别为  $9.18 \mu\text{m}$  和  $9.79 \mu\text{m}$ ;修正后面形平均绝对误差和均方根误差分别为  $0.71 \mu\text{m}$  和  $0.75 \mu\text{m}$ ,提高了面形测量精度,验证了理论分析的正确性及提出的反射率修正算法的有效性。本文的研究内容对光谱共焦位移传感系统测量曲面并提高系统测量精度具有一定指导意义。

关键词:面形测量; 反射率修正; 光谱共焦; 峰值漂移; 柱透镜

## 驻波场中手性粒子的捕获特性研究

白靖 1\*, 刘轩 1, 葛城显 2, 吴振森 3

1 西安邮电大学电子工程学院, 西安 710100;

2 中国电子科技第三十九研究所, 西安 710065;

3 西安电子科技大学物理学院, 西安 710071

摘要: 本文基于麦克斯韦应力张量和广义洛伦兹-米理论, 提出了一种研究双高斯光束对手性粒子捕获力的理论方法。光束以任意方向传播, 利用坐标旋转定理在粒子坐标系中以球矢量波函数(SVWFs)进行扩展。通过对向量场叠加, 得到总入射场的展开系数。根据麦克斯韦应力张量分析, 推导得到手性球体上捕获力的解析表达式。将手性球退化为各向同性介质球时的辐射力结果与文献进行对比, 结果十分吻合, 验证了该理论和程序的准确性。分析了光束参数、粒径参数和手性参数对辐射力的影响。研究表明高斯驻波阱较单高斯光束更容易捕获或限制大尺寸的手性球粒子, 并且驻波阱的稳定俘获对手性参数十分敏感, 采用合适的圆偏振态驻波可能更容易实现对手性球体的轴向捕获。对手性粒子辐射力的理论预测研究是改进光镊技术的有效方法, 可为实现对手性粒子的高精度操作提供有效途径。

关键词: 辐射力, 双光束光阱, 手性粒子, 球矢量波函数

光镊技术由Ashkin 根据激光束捕捉和加速粒子的实验现象发现<sup>[1]</sup>, 其可以在不与粒子发生物理接触的情况下捕捉和操纵活体样品, 因此在分子生物学、物理学和化学工程等领域引起广泛关注。手性介质作为光学活性物质在 19 世纪被首次提出。凭借其独特的光学旋转特性, 手性材料被广泛制造并用于生物医学、微分子操作、物理学和燃料燃烧。在过去的几十年中, 许多研究人员基于不同的分析方法对手性材料和激光束之间的相互作用进行了广泛的研究。研究双高斯光束对球形粒子的辐射作用, 与传统的单光束有很大的不同。特别是对于手性纳米粒子, 需要进一步研究。对任意偏振的双高斯光束对手性纳米粒子的辐射力研究结果可能在显微镜检测和手性结构的操作方面具有潜在的应用价值。鉴于此, 本论文在 GLMT<sup>[2]</sup>的基础上, 推导出任意入射双高斯光束与手性纳米粒子作用的入射场和散射场, 并应用散射结果结合动量守恒理论, 得到任意偏振双激光束对手性球体的横向和轴向辐射力公式, 分析光束和粒子各参数对辐射力分布的数值影响, 以期提高手性粒子的高精度光学捕获性能操作方法的准确性和高效性。

参考文献

[1] Ashkin A, Acceleration and Trapping of Particles by Radiation Pressure[J], Physical Review Letters, 1970, 24(4), 156

[2] Gouesbet G, Lock J A, Rigorous justification of the localized approximation to the beam-shape coefficients in generalized Lorenz-Mie theory. II. Off-axis beams[J], The Journal of the Optical Society of America A, 1994, 11(9), 2516

## 硅基光子集成芯片光纤陀螺

毛玉政

中国航空工业第六一八研究所, 陕西省西安市电子一路 92 号, 710065

Email: myzxjtu@163.com

摘要: 光纤陀螺用于敏感载体旋转角速率, 是武器系统远程控制、定位定向、精确打击的核心传感器之一。但传统光纤陀螺采用分立光纤器件熔接形成光路结构, 陀螺尺寸大、成本高且工艺复杂。未来军用及民用领域对小体积、低成本的光纤陀螺需求巨大, 利用光子集成芯片代替传统光纤分立器件, 可有效减小光纤陀螺尺寸, 借助硅光 CMOS 兼容工艺的大规模批量生产优势, 可大幅降低生产成本, 提高出货量, 这是光纤陀螺发展的必然趋势。本报告主要论述了国内外光子集成芯片陀螺的发展现状及待解决的关键技术难题, 并对团队在硅基光子集成芯片陀螺领域开展的相关工作、取得的成果进行简要介绍, 最后对光子集成芯片陀螺未来的发展进行展望。

关键词: 光纤陀螺; 光子芯片; 有源/无源混合集成; 超细径保偏光纤

## 一种基于铌酸锂环形开口结构的非线性超表面

孙越

(西安工程大学 理学院, 陕西 西安 710065)

17609205265@163.com

摘要: 为了在光学元件结构中实现高效非线性转换, 本文设计了一种由金纳米圆环、开口金环谐振器和四个铌酸锂纳米柱组成的结构单元, 形成了一种复合结构的超表面。利用开口环谐振器和金纳米环共同增强局域电场, 并且采用四个具有高二阶非线性极化率的LiNbO3 介质纳米柱作为二次谐波转换器, 可降低损耗, 提高非线性转换效率。数值模拟计算得到的二次谐波转换效率为 0.16%。该非线性超表面为具有高非线性转

化效率的新型纳米光学器件探索和设计提供了新思路。

关键词:非线性光学; 超表面; 非线性转换; 二次谐波产生

## Thickness-dependent terahertz emission from Bi<sub>2</sub>S<sub>3</sub> films under excitation below and above the band gap

Yayan Xi

School of Physics, Northwest University, Xi'an 710069, China

**Abstract:** Two-dimensional (2D) materials demonstrate fascinating thickness-dependent optical properties due to their van der Waals interaction and quantum confinement in the linear optical regime. However, the thickness-dependent nonlinear optical response is more complicated as virtual carriers (dipoles) and real carriers can be generated by below- and above-band-gap excitation, which calls for a more comprehensive understanding of these carriers in 2D materials. Herein, a direct band gap Bi<sub>2</sub>S<sub>3</sub> is utilized to investigate the thickness-dependent nonlinear optical response by a terahertz (THz) emission spectroscopy. The results suggest that the THz emission intensity decreases with the increase of band gap energy under an 800-nm femtosecond laser excitation, which can be described by an empirical exponential equation. Under below-band-gap excitation, the optical rectification effect induced by instantaneous polarization (virtual carriers) dominates the THz emission mechanism in thin Bi<sub>2</sub>S<sub>3</sub> films. In contrast, under above-band-gap excitation, real carriers are controlled by both resonant optical rectification and surface depletion electric field effects, resulting in shift and drift currents in thick Bi<sub>2</sub>S<sub>3</sub> films. The contribution ratio of the shift and drift currents is  $\sim 1 : 1$  at 45° oblique incidence. This competition between shift and drift currents results in the elliptically polarized THz wave generation, and the major axis orientation and ellipticity of the ellipse could be manipulated by changing the polarization of the pump light. In this paper, we imply the potential for designing tunable on-chip THz sources and nonlinear optoelectronic devices based on thickness-dependent 2D materials.

**Key words:** thickness-dependent Bi<sub>2</sub>S<sub>3</sub> film, optical rectification, shift current, drift current

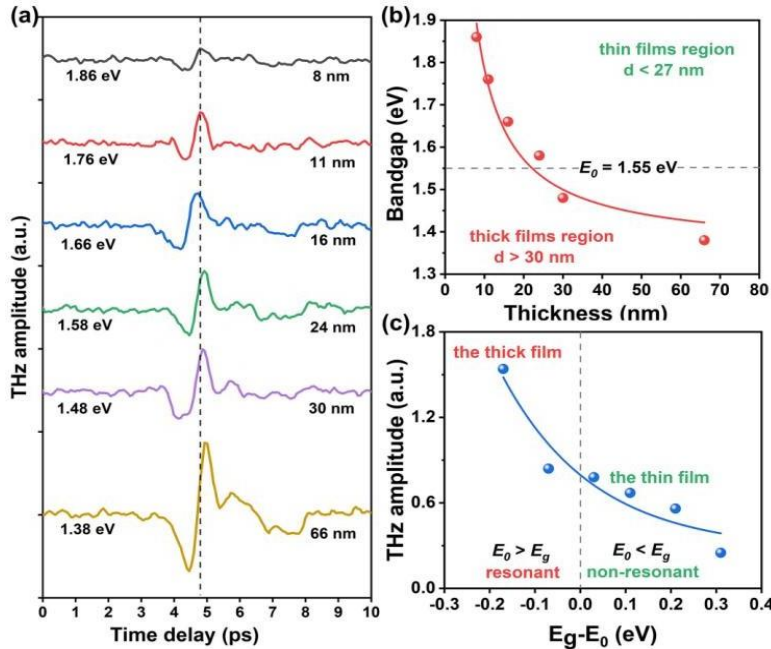


FIG. 1. (a) Time-domain signals of the Bi<sub>2</sub>S<sub>3</sub> films with different thicknesses under p polarization light excitation. (b) Thickness-dependent band gap energies of Bi<sub>2</sub>S<sub>3</sub> films. (c)  $E_0$ - $E_g$ -dependent THz peak-to-valley amplitude. The band gap energies of the representative thick and thin Bi<sub>2</sub>S<sub>3</sub> films are 1.38 and 1.86 eV, respectively.

Thickness is crucial for the fundamental investigation of intrinsic photon responses and optoelectronic properties of two-dimensional (2D) materials [1,2] in the linear optical regime. Nonetheless, the evolution of photocarriers in thickness-dependent nonlinear optical processes is relatively less explored but significant for deepening the understanding of fundamental physics and boosting the development of compact optoelectronic devices based on 2D materials. Herein, we investigate the THz emission properties of band-gap-tunable Bi<sub>2</sub>S<sub>3</sub> films prepared by chemical vapor deposition (CVD) on sapphire substrates. The THz radiation from the thin Bi<sub>2</sub>S<sub>3</sub> film only results from the optical rectification effect. The THz radiation from the thick Bi<sub>2</sub>S<sub>3</sub> film is induced by shift currents attributing to the resonant optical rectification effect and drift currents originating from the surface electric field (SEF) effect.

With the Bi<sub>2</sub>S<sub>3</sub> film thickness increasing from 16 to 66 nm, its band gap energy decreases from 1.86 to 1.38 eV, presenting a thickness-dependent nonlinear optical response. Under below-band-gap excitation, the optical rectification effect induced by instantaneous polarization (virtual carriers) significantly dominates THz emission from the thin Bi<sub>2</sub>S<sub>3</sub> film. Under above-band-gap excitation, the E<sub>X</sub> component of THz radiation from the thick Bi<sub>2</sub>S<sub>3</sub> film is demonstrated to result from the shift current driven by the resonant optical rectification effect with a contribution of 44% and the drift current resulting from the surface depletion electric field effect. In comparison, the E<sub>Y</sub> component mainly originates from the shift current motivated by the resonant optical rectification, which has ~88% contribution to the THz radiation.

References:

- [1] K. Synnatschke, P. A. Cieslik, A. Harvey, A. Castellanos-Gomez, T. Tian, C.-J. Shih, A. Chernikov, E.
- [2] J. G. Santos, J. N. Coleman, and C. Backes, *Chem. Mater.* **31**, 10049 (2019).
- [3] L.-Y. Pan, Y.-F. Ding, Z.-L. Yu, Q. Wan, B. Liu, and M. Q. Cai, *J. Power Sources* **451**, 227732 (2020).

## 放电辅助激光诱导击穿光谱增强特性与应用研究

许博坪

陕西省西安市高新技术产业园信息大道 17 号中国科学院西安光学精密机械研究所  
xuboping2018@opt.ac.cn

摘要:激光诱导击穿光谱 (Laser-induced breakdown spectroscopy, LIBS) 是一种以原子发射光谱法为基础的新型元素分析技术, 具有快速实时检测、原位监测、无需复杂样品预处理等突出优势, 可实现多元素同时远程在线分析。目前, 已被广泛应用于环境检测、深空深海探测、冶金、石油工程等领域。然而, LIBS 技术最大的挑战在于探测痕量元素时光谱强度弱、可重复率小、信噪比 (Signal-to-noise ratio, SNR) 差、探测灵敏度低。因此, 为了进一步提升 LIBS 在痕量领域的探测性能, 提出了一种基于火花放电与电弧放电协同辅助激光诱导等离子体的方法。与传统单脉冲 LIBS 技术相比, 该方法可在维持低放电能耗情况下, 使痕量元素的光谱强度、SNR 增强超过 1 个数量级, 同时极大延长等离子体寿命。痕量探测结果显示, 该方法可将痕量元素检出限降低至亚 ppm 量级。凭借这些优势, 该方法将在各种工业应用中展示出巨大的潜力。

关键词: 放电辅助激光诱导击穿光谱, 光谱增强, 痕量物质探测

## 基于 LK 高斯金字塔的凸集投影距离像超分辨重构方法研究

周绪浪 1, 王春阳 1,2\*, 刘雪莲 1, 施春皓 2, 席贯 1

1. 西安工业大学 西安市主动光电成像探测技术重点实验室, 陕西 西安 710021;

2. 长春理工大学 电子信息工程学院, 吉林 长春 130022

作者 Email: zhouxulang0604@163.com;

导师 (通讯作者) Email: wangchunyang19@163.com;

摘要: 针对目前阵列式激光雷达所成距离像分辨率低, 包含目标细节和边缘信息少的问题, 提出一种结合 Lucas-Kanade (LK) 光流法与高斯金字塔的凸集投影超分辨重构方法。该方法将单帧低分辨率距离像通过最近邻插值得到参考高分辨距离像, 利用 LK 光流法对多帧低分辨率图像进行运动估计并结合高斯金字塔对估计的运动矢量进行修正, 再根据距离像中目标边缘处距离值差异引入梯度约束, 最后计算估计距离值与实际

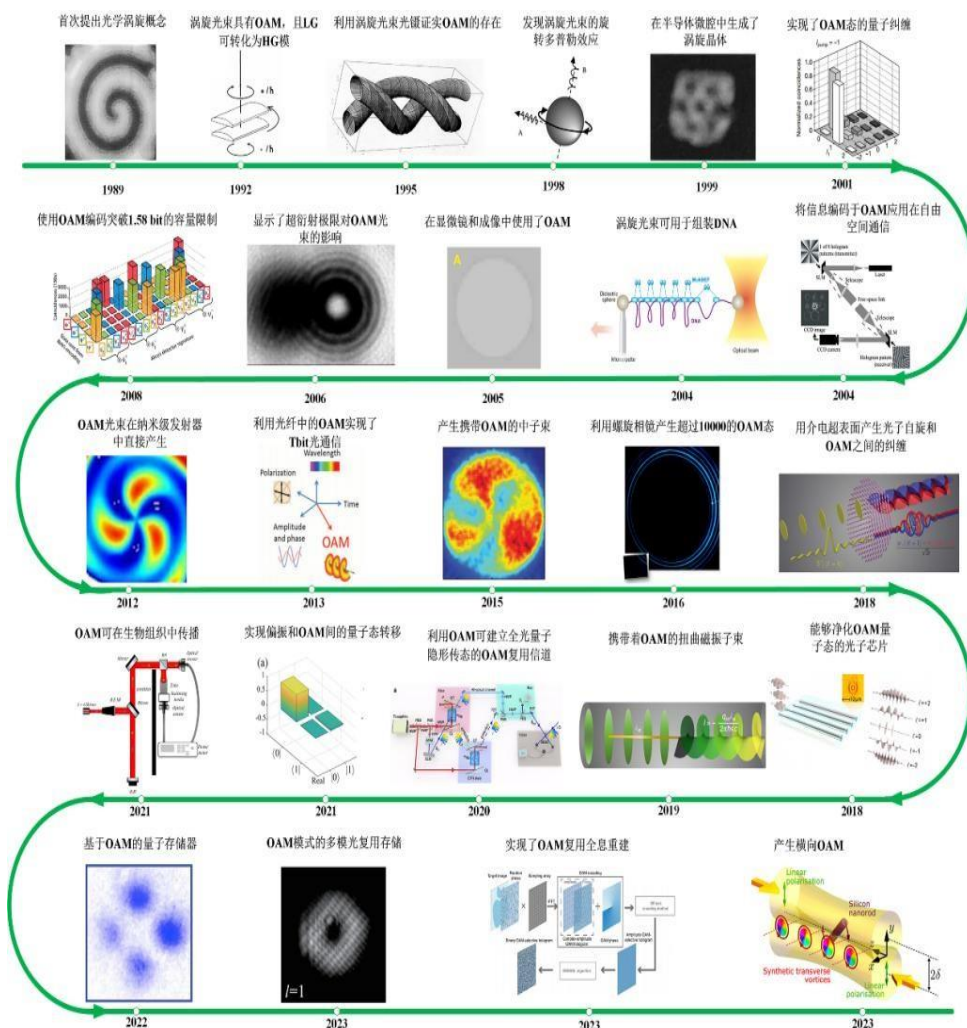


距离值残差，并根据残差利用点扩散函数迭代修正高分辨参考距离像。使用双线性插值、双立方插值、凸集投影、自适应校正阈值的凸集投影与所提方法分别对数据集和实采距离像进行超分辨重构，通过距离像重构效果和客观评价指标来验证所提方法有效性。实验结果表明，所提方法在放大倍数为 2 倍、4 倍、8 倍情况下较插值方法、凸集投影方法指标均有所提升，其中该方法在数据集上平均梯度 (Average Gradient, AG) 较凸集投影方法提升 11.37%，边缘强度 (Edge Intensity, EI) 提升 7.46%；在实采数据上平均梯度提升 11.84%，边缘强度提升 8.4%，证明所提方法在提高距离像分辨率的同时能有效提升重构距离像的细节边缘质量。

关键词:凸集投影; LK 光流法; 高斯金字塔; 超分辨重构; 距离像

### 光子轨道角动量及其在量子计算中的应用研究

张敏, 范亚男, 寇芸洁, 王斐然\*  
 (西安工程大学理学院, 陕西西安 710048)  
 feiran0325@xjtu.edu.cn



摘要:光子轨道角动量由于螺旋相位和高维量子特性,在量子计算方面有着巨大的应用潜力。本文基于目前已有的研究工作,介绍了轨道角动量的重要发展历程以及各领域的相关应用,并给出了基于轨道角动量的量子逻辑门以及其实验实现的相关工作,如高维非门、交换门、控制门等。同时,介绍了几种基于轨道角动量的量子算法。近年来,轨道角动量在量子计算方面的研究成为一大热点,但该领域尚处于发展阶段,还有很多技术和理论上的挑战需要克服。相信随着科技的进步,其在未来具有非常广阔的发展前景。

关键字:量子计算; 光子轨道角动量; 量子逻辑门

基金项目:国家自然科学基金青年科学基金项目(No. 11804271)

## 大气压下氩气脉冲直流放电等离子体射流特性的数值模拟

皇甫浩杰<sup>1</sup>, 高爱华<sup>1</sup> †, 钱程<sup>2</sup> †, 何藩<sup>1</sup>

1. 西北大学物理学院, 西安 710069

2. 西北大学城市与环境学院, 西安 710069

**摘要:**通过数值模拟对准无限大平行平板(间距 0.9 mm)放电装置, 在氩气流速一定、大气压脉冲直流放电情况下的等离子体射流特性进行了研究, 分析了氩气流速和放电电压对等离子体传播特性的影响。结果表明, 等离子体射流在高压电极附近产生, 并沿轴向和径向传播, 轴向在靠近阳极一侧沿 0.96 摩尔分数的氩气-空气混合层传播, 传播速度基本恒定为  $10^4$  m/s, 径向由阳极至阴极沿弧线传播, 前期传播速度慢, 后期较快; 氩气流速越大, 由阳极传播至阴极所需时间越长; 电压越高径向传播越快; 沿轴向传播的电子密度为  $10^{18}$  m<sup>-3</sup> 左右, 沿径向传播的电子密度最大可达  $10^{19}$  m<sup>-3</sup> 左右。电子密度随电压的增加而增加, 但基本不受流速的影响。空气的存在降低了放电开始所需的电压, 这对等离子体射流的形成尤为重要。当氩气处于层流状态时, 流速会影响等离子体初期的传播速度和等离子体的射流长度, 工作电压会影响等离子体的电子密度和传播速度。本工作对基于该结构的离子源提供了理论基础。

**关键词:**大气压放电, 脉冲直流, 等离子体射流, 数值模拟

## 基于反射率修正的柱透镜面形光谱共焦测量研究

李春艳, 刘畅, 刘继红, 李丹琳, 蒋杰伟

(西安邮电大学 电子工程学院, 陕西 西安 710121)

L17829090670@163.com

**摘要:**为实现柱透镜面形的精确测量, 对反射率引起的面形测量误差进行了研究。首先介绍了光谱共焦位移传感系统的工作原理, 并在空间坐标系下利用柱透镜的结构参数, 推导了系统的光谱响应, 建立了柱透镜面形测量模型。然后, 对各点反射率引起的光谱曲线谱峰漂移, 进而造成的面形测量误差进行了理论研究及仿真分析, 为修正透镜曲面反射率对测量结果的影响, 提出采用 S-G 滤波及高斯拟合实现滤波和光谱信号峰值波长的提取, 建立了反射率误差修正算法, 最后通过搭建实验平台, 完成了基于反射率修正的柱透镜面形测量。实验结果表明:修正前面形测量结果的平均绝对误差和均方根误差分别为 9.18 μm 和 9.79 μm; 修正后面形平均绝对误差和均方根误差分别为 0.71 μm 和 0.75 μm, 提高了面形测量精度, 验证了理论分析的正确性及提出的反射率修正算法的有效性。本文的研究内容对光谱共焦位移传感系统测量曲面并提高系统测量精度具有一定指导意义。

**关键词:**面形测量; 反射率修正; 光谱共焦; 峰值漂移; 柱透镜

## 基于泵浦调制技术的调Q 锁模光纤激光器

陈雅妮, 张博媛, 郭若彤, 韩冬冬\*

西安邮电大学, 电子工程学院, 710121

\*handongdong@xupt.edu.cn

**摘要:**本文利用泵浦调制技术展示了一种稳定的调Q 锁模掺铒光纤激光器。在直流泵浦驱动电流下, 实现了连续波锁模操作。之后, 向泵浦驱动中注入调制信号(方波信号)时产生稳定的调Q锁模脉冲。随着调制信号参数(占空比或振幅)的变化, 调Q 锁模脉冲包络的重复频率和时间宽度发生变化。调Q 脉冲形成机制可能是由于泵浦调制引起的腔内增益饱和和可饱和吸收强度的变化, 这些变化会影响积累足够空腔能量所需的持续时间, 从而影响脉冲的时间特性。这项工作为产生调Q 锁模脉冲提供了一个有效的方法。

**关键词:**超快激光技术, 调Q 锁模光纤激光器, 泵浦调制技术, 可饱和吸收体

## Q-switched mode-locked fiber laser based on the pump modulation technique

Yani Chen, Boyuan Zhang, Ruotong Guo and Dongdong Han\*

School of Electronic Engineering, Xi'an University of Posts and Telecommunications, Xi'an 710121, China

**Abstract:** We demonstrated a stable Q-switched mode-locked (QML) erbium fiber laser using pump modulation techniques. Continuous wave mode locked (CML) operation was realized at DC pumping driver current. While the stable QML pulses were generated when a modulation signal was injected

into the pump driver. As the parameters of the modulation signal (duty cycle or amplitude) were varied, the temporal width and repetition rate of the Q-switched pulse envelope could be adjusted. The formation mechanism could be attributed to the change of the intensity of gain saturation and saturable absorption in the cavity caused by the pump modulation. These alterations affect the duration needed to accumulate sufficient cavity energy thus influencing the temporal parameter of the pulse. This work provided an effective way to generate QML pulses.

**Keywords:** Ultrafast laser technology, Q-switched mode-locked fiber laser, Pump modulation technique, Saturable absorbers

### 三格点胞内耦合产生的拓扑态

党煜

西北大学, 西安, 710127

202132890stumail.nwu.edu.cn

**摘要:**这项研究以高斯光诱导的三格点光子晶格为平台,旨在深入探究胞内耦合系数与虚耦合系数对光子结构的影响,进而研究拓扑光子学中的新现象。这一研究的应用前景广泛。首先,它为光子学器件的设计提供了新的可能性,通过调节非循环性参数 $\gamma$ ,可以实现带结构的精细调控,有望用于光波导器件、光调制器和光学传感器等领域。其次,这项研究为拓扑光子学提供了新的材料平台和实验验证,未来或可应用于拓扑绝缘体激光器和拓扑光电调制器的开发。此外,通过调节带结构,还可优化光传输的速度和方向,为信息传输和处理领域提供更高效的解决方案。最后,这些拓扑结构还有望应用于量子光学实验,为光子的量子态制备和操控提供新的工具和平台。未来的研究方向包括寻找更强非循环性的材料系统、进行实验验证、进行更复杂的多尺度建模和仿真,以及探索拓扑结构与其他功能性材料的结合,实现多功能光子器件的开发。这项研究为光子学和拓扑光子学领域的进一步发展提供了有趣的见解和前景。

**关键词:**三格点,光传输,虚耦合,拓扑态

### 1.6- $\mu\text{m}$ Single-Frequency Erbium-doped Fiber laser based on a FP-FBG Filter and two cascaded Sub-Rings

*Yaqi Zhai*

Northwest University, Xi'an 710127 zhaiyaq@163.com

**Abstract:** We proposed and demonstrated a single-frequency erbium-doped fiber laser (EDFL) based on a Fabry-Perot Fiber Bragg Grating (FP-FBG) and two cascaded sub-rings (TCSR). A narrower bandwidth fiber Bragg grating was used to determine the operating wavelength of the laser at 1600.06 nm, which was combined with a FP-FBG as well as TCSR device to achieve stable single longitudinal mode operation. In addition, the design and fabrication methods of TCSR filters were described in detail, and the selection principles of SLM were analyzed. The experimental results showed that the optical signal-to-noise ratio (OSNR) of the output laser was greater than 73 dB, and the linewidth was measured of 435 Hz by using the short-delayed self-heterodyne measurement method. Within an hour of continuous monitoring, the maximum variation of center wavelength and optical power were 0.09 nm and 0.169 dB, respectively. The single longitudinal mode state of the laser was verified using the self-homodyne method, and no mode-hopping phenomenon was found within 60 min of observation, indicating that the laser has good stability.

**Key Words:** erbium-doped fiber laser (EDFL)、Fabry-Pérot filter、two cascaded sub-rings(TCSR)

### All-PM Yb-doped mode-locked fiber laser with high single pulse energy and high repetition frequency

*Chaohui Fu, Baole Lu, Jintao Bai*

Northwest University, Xi'an 710127

**Abstract:**We demonstrate an all-polarization-maintaining (PM) ytterbium (Yb)-doped fiber

laser with a figure-of-9 structure to generate mode-locked pulses with high single pulse energy and high repetition frequency. By exploiting the saturable absorption effect of the nonlinear amplifying loop mirror (NALM), a stably self-started mode-locking operation is achieved with a spectrum bandwidth of 13 nm and a pulse duration of 4.53 ps. The fundamental frequency is 97.966 MHz at the maximum output power of 143 mW in single pulse mode-locked operation, corresponding to the single pulse energy is 1.46 nJ. The output pulses maintain both high repetition frequency and high single-pulse energy. To the best of our knowledge, this is the highest single-pulse energy achieved in the short cavity. Moreover, the superior stability of the mode-locked operation was measured in 45 minutes. This laser oscillator can be an ideal seed source for applications such as high-energy amplifiers.

**Key Words:** fiber laser, mode-locked laser, all-PM laser, high single pulse energy, high repetition frequency.

## 高维焦散光束的机理研究

管佳豪, 何云东, 仝珍珠, 薛少杰, 齐新元\*

西北大学, 西安, 710127

qixycn@nwu.edu.cn

摘要:激光自诞生以来就凭借着高单色性、高方向性、高相干性以及高能量四大特性在医疗、生物、制造、通信等领域得到了快速的发展。绝大多数激光器的典型输出模式是基模高斯光束,这也是应用最广泛的激光模式。随着激光应用的不断发展,高斯激光模式已经无法满足科学技术的要求,为此研究人员通过调制光场的空间振幅、相位以及偏振态分布,将传统的基模高斯光束转换为具有独特空间分布的光场,如无衍射光场,自加速光场,自聚焦与自散焦光场,涡旋光场以及矢量光场等。它们具有很多新颖的光学特性,如无衍射特性、自加速特性、自愈特性、超衍射极限聚焦以及自旋轨道角动量耦合等。

一类受到广泛关注的结构光场是所谓的无衍射光束或传播不变光束。其中,研究最为广泛也是最先在实验中产生的自加速光束是艾里光束,它和贝塞尔光束一样具有无衍射的光学特性,此外艾里光束还具有令人惊讶的自加速特性,在自由空间中沿着一条抛物线加速传播。艾里光束自加速的特性打破激光束沿直线传播的传统观念,同时也激发了研究人员对各种自加速光束进行了深入的研究。自加速光束能够沿着弯曲的轨迹传播已经成为共识,然而弯曲的轨迹并不是指光线的路径也不是光束的质心(这些在自由空间中只能沿着直线传播)而是焦散。焦散是光线汇聚的点、线、曲面等,也就是光线族的包络,同时光束强度的局域最大值对应焦散的位置,并表现为弯曲的轨迹。实际上,艾里光束的自加速轨迹就是其焦散曲线。另一个具有独特焦散结构的光束是皮尔斯光束,其横截面的焦散结构是一条尖点曲线,皮尔斯光束具有传播形式不变、自聚焦以及自愈的特性。光学中的焦散是突变的具体表现,在控制参数维度不大于4时只存在七种基本突变,按照控制空间维度增加的顺序分别为:折叠、尖点、燕尾、蝴蝶、椭圆脐带、双曲脐带、抛物脐带。在光学中每种突变会形成一种稳定的衍射光场我们称之为衍射突变光场。突变理论描述了外界条件的平滑变化所导致系统状态的突然改变<sup>[1, 2, 3, 4]</sup>。在光学中,波前的平滑变化会改变光线的方向,使不同的区域光线相交的次数突然改变,突然变化的临界点便是突变结构。在控制参数为一维时,对应着折叠突变的是具有抛物线轨迹的艾里光束。以折叠焦散为界,其中一侧存在两条光线相互干涉,而另一侧则不存在光线。在二维空间中,对应尖点突变的是皮尔斯光束,以尖点突变为界上下两侧发生干涉的光线数量是不同的,尖点下方相互干涉的光线是三条,而尖点上方则仅有一条光线。衍射突变光束因具有独特的焦散结构故而可以用来设计具有特殊空间结构的光束,然而目前只涉及到低维突变。通常来说高阶的突变会包含低阶的突变,因此随着阶次的增加,衍射突变光束会展现出新的光学特性。7种基本的衍射突变光束如同组成物质的原子,深入探索这7种基本衍射突变光束才能设计出具有任意复杂焦散的衍射突变光场,并且进一步在微加工、粒子操控、显微成像等领域带来全新变革。而目前高阶的衍射突变光束却少有研究,其独特的光学特性也不为人知。因此,设计高阶衍射突变光束具有重要的研究意义与价值。

参考文献

- [1] Berry, Michael V. and Colin Upstill. "IV Catastrophe Optics: Morphologies of Caustics and Their Diffraction Patterns." *Progress in Optics* 18 (1980): 257-346.
- [2] Arnold, V. I. Catastrophe theory [M]. Springer Science & Business Media, 2003.
- [3] Zeeman E C. Catastrophe Theory [J]. Springer, 1976, 196(4): 65-83.
- [4] Kravtsov Y A, Orlov Y I. Caustics, catastrophes and wave fields [M]. Springer Science & Business Media, 2012.

## 基于自适应遗传算法的自动锁模光纤激光器

郭若彤, 陈雅妮, 张博媛, 韩冬冬\*  
西安邮电大学, 电子工程学院, 710121  
[\\*handongdong@xupt.edu.cn](mailto:*handongdong@xupt.edu.cn)

**摘要:**在本研究中, 针对基于非线性偏振旋转的掺铒光纤激光器的自动锁模操作, 提出并实现了一种改进的自适应遗传算法。该算法将遗传算法与自适应交叉率和突变率相结合, 随着算法运行过程中迭代次数的增加, 交叉率和突变率随着适应度函数值的变化动态调整。当改进自适应遗传算法不断优化, 将腔内偏振态收敛到目标状态时, 会自动产生一个展宽脉冲。从其他状态调节到展宽脉冲锁模所需平均锁模代数为 2 代。还研究了超快掺铒光纤激光器在遗传算法控制下, 不同参数结构 (包括交叉率和突变率) 的演化曲线, 证明了改进自适应遗传算法的有效性。本工作为实现自动锁模光纤激光器的快速偏振搜索提供了一个新的方案。

**关键词:** 自适应遗传算法, 展宽脉冲, 被动锁模光纤激光器

## Adaptive genetic algorithm-based automatic mode-locked fiber laser

*Ruotong Guo, Yani Chen, Boyuan Zhang, Dongdong Han\**

School of Electronic Engineering, Xi'an University of Posts and Telecommunications, Xi'an  
710121, China

**Abstract:** A modified adaptive genetic algorithm (GA) is proposed and implemented in a nonlinear polarization rotation based mode-locked erbium-doped fiber laser (EDFL). The algorithm combines a GA with adaptive crossover rate and mutation rate. With the increase of iterations in the process of solving operation, the crossover rate and mutation rate are dynamically adjusted with the change of the fitness function value. A stretched pulse was automatically generated when the modified adaptive GA was continuously optimized to converge the intracavity polarization state to the target state. The average generations required to adjust from other states to stretched pulse locking is 2 generations, which is superior to the general GA. The evolution curves of mode-locked EDFL with different crossover and mutation rates were also investigated, demonstrating the effectiveness of the proposed modified adaptive GA. This work provides a new scheme for fast polarization searching in an automatic mode-locked fiber laser.

**Keywords:** Adaptive genetic algorithm, stretched pulse, passively mode-locked fiber

## 自聚焦光束的调控机理研究

何云东, 仝珍珠, 管佳豪, 薛少杰, 齐新元\*  
西北大学, 西安, 710127 [qixycn@nwu.edu.cn](mailto:qixycn@nwu.edu.cn)

**摘要:**光场调控、传输及应用是当前国际光学与光子学领域的一个研究热点。目前主要是指调控光场振幅、偏振态、相位、空间相干结构等空间分布, 以产生具有特殊空间分布的新型光场。产生的新型光场拥有一些良好的光学特性, 比如无衍射传播、自聚焦和自愈等。自聚焦光束 (autofocusing beams) 是指一类在保持低能量传播一定距离后在某一处能将能量汇聚于一点的光束。2021 年, Bongiovanni 等人提出了一种新的自聚焦光束——钉状涡旋光。这种径向对称的自加速光束可以表现出低强度传播, 并在目标前方具有可控的突然自动聚焦, 随后振幅重塑为高阶贝塞尔类光束, 空心半径和环形主瓣宽度随传播距离而变化。通过施加适当设计的振幅调制, 可以很容易地控制峰值强度的变化, 并且还可以携带轨道角动量。同时其在一定距离内能够抵消衍射。这些光学特性使其在材料消融、医疗手术、生物医学成像、粒子操纵和自由空间光学通信都有潜在用途。但目前这种光束仍存在传输距离较短, 能量向四周扩散较多的问题, 这就需要一种简单、通用的方法来自由操纵光束长度、直径和轴向强度分布, 而准随机空间复用相位掩模恰好可以解决上述问题。传统上, 光束的轴向强度的平坦化需要对入射光束的相位和振幅进行调制, 本课题通过使用准随机空间复用相位掩模, 在特定轴向位置创建多个焦点来控制光束长度, 优化焦点位置以使钉状涡旋光束轴向强度分布变平, 并且随机空间复用抑制了高阶衍射, 因此不需要使用空间滤波器, 使光学系统更为紧凑。

**关键词:** 自聚焦光束、相位掩膜、相位、振幅

## Self-sweeping regimes control in a bi-directional Yb-doped ring fiber laser

Xianming Huang,<sup>1,2</sup> Chengcheng Lu,<sup>1,2</sup> Zhenzhong Zuo,<sup>1,2</sup> Haowei Chen,<sup>1,2</sup> Baole Lu,<sup>1,2\*</sup> and Jintao Bai<sup>1,2</sup>

<sup>1</sup>State Key Laboratory of Energy Photon-Technology in Western China, International Collaborative Center on Photoelectric Technology and Nano Functional materials, Institute of Photonics &

Photon-technology, Northwest University, Xi' an 710127, China

<sup>2</sup>Shaanxi Engineering Technology Research Center for Solid State Lasers and Application, Shaanxi Provincial Key Laboratory of Photo-electronic Technology, Northwest University, Xi' an 710127, China

\*Corresponding author: [lubaole1123@163.com](mailto:lubaole1123@163.com)

**Abstract:** We report three self-sweeping regimes in a single-mode bi-directional Yb-doped ring fiber laser with increasing pump power: normal self-sweeping operation, wavelength stationary state, and reverse self-sweeping operation. The intensity dynamics of both normal and reverse self-sweeping are a dual-longitudinal-mode quasi-continuous wave formed by alternating the flat and burst regions. In addition, the wavelength stationary state can be achieved at an arbitrary value between 1067.5 nm and 1072.3 nm, depending on the historical process of wavelength self-sweeping, whose intensity dynamics consist of chaotic pulses and periodic bursts. In short, switching wavelength self-sweeping regimes can be achieved simply by changing the pump power. These research results are potentially valuable for developing and applying self-sweeping fiber lasers.

**Keywords:** self-sweeping fiber laser; tunable laser; dual-longitudinal-mode; quasi-continuous wave

## TiO<sub>2</sub> spatially confined growth of Sb<sub>2</sub>(S,Se)<sub>3</sub>@TiO<sub>2</sub> NTs heterojunction photoanodes and their photoelectrochemical properties

Wei Jin, Xiaoyun Hu, Hui Miao\*

School of Physics, Northwest University, Xi' an, Shaanxi 710127, PR China

\*E-mail: [huim@nwu.wdu.cn](mailto:huim@nwu.wdu.cn)

**Abstract:** Titanium dioxide (TiO<sub>2</sub>), a conventional n-type semiconductor, was widely used in photocatalysis, electrocatalysis and photoelectrocatalysis due to its good UV absorption and stable physical and chemical properties. However, its wide band gap and low oxygen reaction (OER) activity limited its application in photoelectrochemical (PEC) water splitting. Antimony selenide sulfide (Sb<sub>2</sub>(S,Se)<sub>3</sub>), as a quasi-one-dimensional photo-absorbing material with adjustable band gap (1.1~1.8 eV) and the advantages of both antimony sulfide (Sb<sub>2</sub>S<sub>3</sub>) and antimony selenide (Sb<sub>2</sub>Se<sub>3</sub>), can better broaden the light absorption range of TiO<sub>2</sub>. In this work, we successfully constructed type-II Sb<sub>2</sub>(S,Se)<sub>3</sub>@TiO<sub>2</sub> core-shell heterojunction, which broadened the TiO<sub>2</sub> light absorption range and effectively promoted the photogenerated carriers separation, transportation and utilization. Of particular note, novel Sb<sub>2</sub>(S,Se)<sub>3</sub> nanospheres (NSPs) (ca. 69 nm) were in-situ grown inside the tubes attributed to the unique space-confinement effect of TiO<sub>2</sub> nanotubes (NTs). The IPCE value for Sb<sub>2</sub>(S,Se)<sub>3</sub>@TiO<sub>2</sub> at 734 nm was 6.53% compared to 0.03% for TiO<sub>2</sub>. The onset potential was moved negatively by 60 mV, and the maximum photocurrent density of 1.53 mA cm<sup>-2</sup> at 1.23 V vs. RHE was 13.9 times higher than that of TiO<sub>2</sub> (0.11 mA cm<sup>-2</sup>). This work provided a new idea for the application of TiO<sub>2</sub> in the field of PEC water splitting.

In this work, TiO<sub>2</sub>/Sb<sub>2</sub>(S,Se)<sub>3</sub> core-shell heterojunction photoanodes were successfully prepared and used in the field of photoelectrochemical water splitting. Based on the space-confinement effect of TiO<sub>2</sub> NTs, smaller nano-sized Sb<sub>2</sub>(S,Se)<sub>3</sub> NPSs (69 nm) were grown in-situ on TiO<sub>2</sub> NTs by hydrothermal method, which was used to broaden the range of light absorption of TiO<sub>2</sub>. In addition, this small-sized and dense

nanostructure of  $\text{Sb}_2(\text{S,Se})_3$  NPSs were used as a light trap structure, which can significantly improve the absorption of light and increase the electrochemical surface active sites of  $\text{TiO}_2$  NTs. At the same time,  $\text{TiO}_2$  NTs also acted as an electron transport layer and reduced the photogenerated carrier recombination rate on the  $\text{Sb}_2(\text{S,Se})_3$  surface. As a result, the significant improvement in the PEC performance can be attributed to the space-confinement effect of  $\text{TiO}_2$  NTs leading to the formation of  $\text{Sb}_2(\text{S,Se})_3$  NPSs photo-trap structures and the efficient separation, transport, and utilization of photogenerated carriers.

**Keywords:**  $\text{TiO}_2$ ,  $\text{Sb}_2(\text{S,Se})_3$ , space-confinement, photoelectrochemical properties

## The mechanism of noise-like pulse in all-normal dispersion all-fiber laser based on nonlinear polarization rotation

*Jiajing Lang*

Northwest University 710127 18131996718@163.com

**Abstract:** Noise-like pulse (NLP) is an interesting phenomenon in lasers, we investigate in detail the mechanism of changing the intracavity polarization state to generate NLP in the all-normal dispersion (ANDi) all-fiber laser based on nonlinear polarization rotation (NPR). Through numerical simulations, we find that changing the intracavity polarization state alters the intracavity transmission state, which in turn affects the positive and negative feedback states in the cavity, enabling the evolution of dissipative soliton (DS) to NLP. To verify the feasibility of the experiment, we built an ANDi all-fiber laser based on NPR, in which filter is a birefringent fiber filter consisting of polarization maintaining fiber with polarization devices, which simplifies the experimental setup and enables wavelength switching. In the experiment, wavelength switching and DS and NLP switching are achieved by rotating the polarization controller to change the polarization state in the cavity. The experimental results are in good agreement with the numerical predictions. This study deepens the understanding of the mechanism of NLP generation by changing the intracavity polarization state in ANDi all-fiber lasers based on NPR, contributes to the design of lasers generating different types of pulses, and is promising for a wide range of applications in the field of supercontinuum spectrum generation.

**Key Words:** Noise-like pulses, dissipative solitons, wavelength switching, fiber lasers.

## 基于拓扑光子晶体环形谐振器的无源光学陀螺仪的理论研究

李港, 万鑫, 彭晨阳, 马春林, 齐新元\*

西北大学, 西安, 710127

qixycn@nwu.edu.cn

**摘要:**陀螺仪作为一种重要的惯性导航设备和姿态控制器, 已经广泛用于无人机、飞行器、导弹等领域。光子晶体陀螺仪(Photonic crystal Gyroscope)是基于萨格纳克(Sagnac)效应<sup>[1]</sup>的谐振式光学陀螺(Resonant Micro-Optical Gyros), 它是通过环路中沿顺时针方向传播光束的谐振频率之差实现对外界角速率的测量。而光子晶体谐振腔是光子晶体陀螺仪的核心敏感元件, 其光学特性与陀螺系统的性能密切相关。目前可以通过集成光学技术、微纳加工技术和新型材料的应用来将光子晶体谐振腔进行小型化和集成化, 提高系统的性能指标。拓扑光子学<sup>[2]</sup>有着基于内在属性的鲁棒性, 可以抵抗各种程度的无序和扰动。这种能力可以使器件很好地工作在各种复杂环境下。光学拓扑器件独特的能耗低, 单向传输, 免疫干扰的特性在光学器件发展上具有巨大研究价值。本课题提出基于二维拓扑谷光子晶体环形腔的更高的Q 因子和低模式体积等优点, 进一步优化陀螺仪对超灵敏旋转测量的性能指标。

**关键词:**光子晶体陀螺仪、拓扑光子晶体谐振腔、角速率、谐振频率

参考文献

[1] Post E J. Sagnac Effect[J]. Reviews of Modern Physics, 1967, 39(2): 475-493.

[2] Ozawa T, Price H M, Amo A, et al. Topological photonics[J]. Reviews of Modern Physics, 2019, 91(1).

## 基于共轭涡旋光干涉的皮米级位移测量方法

李孟昊<sup>a</sup>, 贾傲驰<sup>a</sup>, 任凯利<sup>a\*</sup>

<sup>a</sup>School of Electronic Engineering, Xi'an University of Posts & Telecommunications, Xi'an 710121, China.

renkaili@xupt.edu.cn

**摘要:**干涉测量常用于图例位移等几何参量的高精度测量。本研究提出基于共轭涡旋光的皮米级位移测量方法,通过螺旋光纤光栅替代空间光调制器实现光场调控,获得共轭涡旋光干涉图像。进一步解调位移前后干涉图样变化,提取图样上所有像素点的光强信息。寻找每一干涉图样的光强最大值,并选取其对应点构成类圆环,解调出微位移参量。通过解调干涉图样光场分布,借助 MATLAB 处理光场信息,并将所得图样信息绘制在极坐标系下,从而实现对旋转角的精确提取。借助本方法处理不同波长图样下的干涉光强图样信息,测算待测图样全行程旋转角度计算其位移量。该项研究为共轭涡旋光干涉的皮米级高精度位移测量的创新设计提供了一种可行的方案。

**关键词:**共轭涡旋光, MATLAB, 图像信息处理, 位移测量

## Topological states switching and group velocity control in two dimensional non-reciprocal Hermitian photonic lattice

Yu Lin, Yuandan Wang, Junhao Yang, Yixuan Fu, Xinyuan Qi \*

School of Physics, Northwest University, 710127, Xi'an, China

**Abstract:**We constructed a two-dimensional photonic lattice with non-reciprocal complex number coupling coefficients. Theoretically and numerically, we studied the system's topological states and group velocity control. The results show that the movement and breaking of Dirac points exist in the energy band of the system. By changing the coupling coefficients, the conversion between Topological states of different Chern numbers, and even topological trivial states can be realized. Topological edge states exist in both Topological states of different Chern numbers systems. Besides, it is also found that both the coupling coefficient and the wave vector can cause the oscillation of the pulse group velocity. At the same time, the topological state can suppress the amplitude of the group velocity profiles. Our findings enrich the theory of light wave manipulation in high-dimensional photonic lattices and provide a novel view for realizing linear localization and group velocity regulation of light waves, which has potential application in high-speed optical communication and quantum information fields.

**Keywords:** Dirac point, imaginary coupling, Chern number, group velocity References

## 原位 Se 化构建 S 型 Sb<sub>2</sub>S<sub>3</sub>@CdSe<sub>x</sub>S<sub>1-x</sub> 核壳异质结及其光电化学特性

刘德康<sup>a</sup>, 张文静<sup>a</sup>, 刘鑫阳<sup>a</sup>, 王屹山<sup>b</sup>, 胡晓云<sup>a</sup>, 苗慧<sup>a\*</sup>

<sup>a</sup> 西北大学物理学院, 西安, 710127

<sup>b</sup> 瞬态光学与光子技术国家重点实验室, 西安, 710119

\*E-mail: huim@nwu.edu.cn

**摘要:**近年来随着能源与环境问题日益严重,太阳能材料已被广泛开发并应用于可再生能源的生产<sup>[1]</sup>。窄带隙半导体 Sb<sub>2</sub>S<sub>3</sub> 由于具有较高的光吸收系数以及合适的禁带宽度被广泛应用于太阳能电池领域<sup>[2,3]</sup>,其在光电化学领域的研究尚处于起步阶段,深能级缺陷较多严重制约其光生载流子高效分离和光电转化效率显著提升。本文采用气相输运沉积法、化学浴沉积法和原位 Se 化法,在 FTO 基底表面制备得到 S 型 Sb<sub>2</sub>S<sub>3</sub>@CdSe<sub>x</sub>S<sub>1-x</sub> 核壳准一维异质结复合光阳极。研究表明:CdSe<sub>x</sub>S<sub>1-x</sub> 纳米颗粒均匀地包覆于棒状 Sb<sub>2</sub>S<sub>3</sub> 表面,复合光阳极在 1.23 VRHE 外加偏压下,光电流密度为 1.53 mA/cm<sup>2</sup>,是单体 Sb<sub>2</sub>S<sub>3</sub> 光阳极 0.61 mA/cm<sup>2</sup> 的 2.5 倍,并使暗电流得到有效降低。在 600 s 的开关光稳定性测试中表现出良好的稳定性与较快的光电流响应特性。分析认为:① 构建形成的 S 型异质结有效解决了 Sb<sub>2</sub>S<sub>3</sub> 深能级缺陷导致其光生载流子严重复合的弊端,实现光生电子与空穴的空间分离;② [hk1]取向的 Sb<sub>2</sub>S<sub>3</sub> 纳米棒和形成的准一维异质结构促进了载流子的高效传输;③ Se 的引入有效调控了 CdS 的能带结构,减缓了 S 的光腐蚀,实现光电极稳定性的显著提升。



升。

关键词:硫化锑, 气相输运沉积法, 原位Se 化, S 型异质结, 光电化学特性

参考文献

- [1] T. Hisatomi, K. Domen, Nat. Catal., 2, 387-399(2019)
- [2] R. Tang, X. Wang, W. Lian, et al., Nat. Energy, 5, 587-595(2020)
- [3] W. Lian, C. Jiang, Y. Yin, et al., Nat. Commun., 12, 3260(2021)

## Epitaxial growth strategy for construction of Tm<sup>3+</sup> doped and [hk1] oriented Sb<sub>2</sub>S<sub>3</sub> nanorods S-scheme heterojunction with enhanced photoelectrochemical performance

*Xinyang Liu, Xiaoyun Hu, Hui Miao\**

School of Physics, Northwest University, Xi'an, Shaanxi 710127, PR China  
huim@nwu.edu.cn (H. Miao)

**Abstract:** Sb<sub>2</sub>S<sub>3</sub> as a light-harvesting material has gradually attracted the attention of researchers in the field of photoelectrocatalysis. The Sb<sub>2</sub>S<sub>3</sub> crystal is composed of parallel one-dimensional (1D) (Sb<sub>4</sub>S<sub>6</sub>)<sub>n</sub> nanoribbons held together resulting in a preferred anisotropic growth. However, The presence of detrimental deep-level defects and low carrier transport efficiency limit further improvements in the PEC performance of Sb<sub>2</sub>S<sub>3</sub>-based photoelectrodes. Current research work on Sb<sub>2</sub>S<sub>3</sub> has focused on the construction of 1D nanostructures and the passivation of deep-level defects to improve its photoelectrochemical properties. In this work, we have successfully constructed SnSe<sub>2</sub>/Sb<sub>2</sub>S<sub>3</sub>: Tm<sup>3+</sup> composite photocathode by chemical vapor deposition (CVD) and hydrothermal method. The surface [hk1] orientation properties of 2D SnSe<sub>2</sub> nanosheets can induce the epitaxial growth of Sb<sub>2</sub>S<sub>3</sub>: Tm<sup>3+</sup> nanorods along the (Sb<sub>4</sub>S<sub>6</sub>)<sub>n</sub> nanoribbons, and the resulting one-dimensional nanorod structure can act as a fast transport channel to facilitate carrier spatial transportation. This is a novel method to optimize the structure of Sb<sub>2</sub>S<sub>3</sub>. The resulting SnSe<sub>2</sub>/Sb<sub>2</sub>S<sub>3</sub>: Tm<sup>3+</sup> S-scheme heterojunction suppressed carrier recombination, providing a stronger driving force in the reaction dynamics to optimize carriers interfacial transportation. Moreover, a novel Tm<sup>3+</sup> doped hydrothermal strategy provided an effective way to weaken the Fermi level pinning effect. The injection efficiency of the optimized SnSe<sub>2</sub>/Sb<sub>2</sub>S<sub>3</sub>: Tm<sup>3+</sup> photocathode is increased to 81.7% and the photocurrent density increased to -0.91 mA cm<sup>-2</sup>, which is 18.2 times higher than that of pristine Sb<sub>2</sub>S<sub>3</sub> photocathode. Our work provides a construction of Tm<sup>3+</sup> doped Sb<sub>2</sub>S<sub>3</sub>-based composite photocathode with dominant growth orientation by a novel epitaxial growth method, which is expected to accelerate the development of Sb<sub>2</sub>S<sub>3</sub> in the field of PEC hydrogen production.

**KEYWORDS:** S-scheme heterojunction; Fermi level pinning; doping strategy; epitaxial growth; photoelectrochemical performance

## Process development and monitoring in stripping of a C45E4 steel plate surface corrosion with 200 ns pulsed fiber laser

*XueChen Liu<sup>1</sup>, Yang Bai<sup>1,2</sup>, RongWei Zha<sup>1</sup>*

1. Institute of Photonics & Photon-Technology, Northwest University, Xi'an 710127, China

2. Shaanxi Engineering Technology Research Center for Solid State Lasers and Application, Xi'an 710127, China

**Abstract:** The effects of average laser power, spot overlap rate and cleaning time on cleaning quality and efficiency were investigated. A laser cleaning online monitoring system was established, and the cleaning degree of the cleaned metal surface was calculated using image recognition technology. By analyzing the change rule of cleanliness under different parameters, a suitable combination of process parameters was optimized. Through the laser-induced plasma

spectroscopy to monitor the small area cleaning process, dynamically adjust the cleaning time of different thicknesses of corrosion layer. High-quality automatic laser cleaning was realized, with the cleaning degree reaching 99.1%, the roughness reaching  $1.45\ \mu\text{m}$ , and the surface oxygen content reaching the oxygen content of the substrate surface.

**Keywords:** Laser cleaning; Rust layer; On-line monitoring technology

In this work, image processing technology was used to study the change rule of cleaning times and cleaning degree of C45E4 mild steel plate with larger area of  $30\ \text{mm} \times 30\ \text{mm}$  under different spot overlapping rate, and the optimal spot overlapping rate of 50% was obtained. LIPS analysis was used to study the Pearson correlation coefficient of  $0.47\ \text{mm} \times 0.47\ \text{mm}$  micro-area C45E4 mild steel plate with the change of cleaning times, and the optimal number of times of cleaning was obtained under different thicknesses of corrosion layer. On this basis, the image processing method is used in conjunction with the LIPS analysis method, and the LIPS analysis method can dynamically correct the minimum number of cleaning times according to the thickness of the corrosion layer of the micro-area, making up for the defects of the image processing method that can not accurately control the laser cleaning process, and 99.1% of the degree of cleanliness shows that the two methods of the two methods work together on the large-area laser cleaning of C45E4 low-carbon steel plate process for effective monitoring.

#### References

- [1] Beklemyshev V. I., Makarov V. V., Makhonin I. I., et al. Photodesorption of metal ions in a semiconductor-water system. *Toxicology & Applied Pharmacology*, 1987, 101(3): 481-483.
- [2] Tam A. C., Leung W. P., Zapka W., et al. Laser-cleaning techniques for removal of surface particulates. *Journal of Applied Physics*, 1992, 71(7): 3515-3523.
- [3] Lu Y. F., Takai M., Komuro S., et al. Surface cleaning of metals by pulsed-laser irradiation in air. *Applied Physics A*, 1994, 59(3): 281-288.
- [4] Renzo S., Roberto P., Salvatore S. A variable pulse width Nd:YAG laser for conservation. *Journal of Cultural Heritage*, 2003, 4(1): 72-76.
- [6] Osticioli I., Siano S., Veiko V. P., et al. Dependence of Nd:YAG laser derusting and passivation of iron artifacts on pulse duration. *Fundamentals of Laser Assisted Micro-and Nanotechnologies*, 2013.
- [7] Wang Zemin, Zeng Xiaoyan, Huang Weiling. Parameters and surface performance of laser removal of rust layer on A3 steel. *Surface & Coatings Technology*, 2003, 166(1): 10-16.

## 具有径轴向的S型Sb<sub>2</sub>S<sub>3</sub>/In<sub>2</sub>Se<sub>3</sub>异质结光电极的构建及其光电化学性能的研究

马震<sup>a</sup>, 胡晓云<sup>a</sup>, 苗慧<sup>a,\*</sup>

<sup>a</sup> 西北大学物理学院, 西安, 710127

<sup>b</sup> 瞬态光学与光子技术国家重点实验室, 西安, 710119

E-mail: huim@nwu.edu.cn

**摘要:** Sb<sub>2</sub>S<sub>3</sub> 是一种典型的窄带隙半导体, 带隙约为 1.7 eV, 具有高吸收系数、长载流子扩散长度和优异的载流子迁移率等优点, 是一种非常有前途的材料。然而, 由于 Sb<sub>2</sub>S<sub>3</sub> 存在严重的光腐蚀现象、许多深能级缺陷以及电子空穴易复合等问题, 它尚未得到充分利用<sup>[1]</sup>。本工作采用气相输运沉积法和水热法构建了一个具有准一维棒状结构的 S 型 Sb<sub>2</sub>S<sub>3</sub>/In<sub>2</sub>Se<sub>3</sub> 异质结, 有效解决了 Sb<sub>2</sub>S<sub>3</sub> 深能级缺陷导致其光生载流子严重复合的弊端, 实现光生电子与空穴的空间分离<sup>[2]</sup>。研究表明, [hk1]取向的 Sb<sub>2</sub>S<sub>3</sub> 纳米棒和沿着 Sb<sub>2</sub>S<sub>3</sub> 径轴向生长的 In<sub>2</sub>Se<sub>3</sub> 异质结促进了载流子的高效传输, 复合光阴极在 0 VRHE 外加偏压下, 光电流密度约为  $2.902\ \text{mA}/\text{cm}^2$ , 是纯 Sb<sub>2</sub>S<sub>3</sub> 单体的 39.22 倍, 并使得暗电流和瞬态尖峰得到了有效的改善。在 210 s 的开关光测试中表现出良好的稳定性, 阻抗图中表现出较小的电荷转移电阻, 注入分离图中表现出较高的电荷注入和分离效率。本工作为 [hk1] 优势晶向的硫化锑光电极的制备提供了一种方法, 通过使用安全, 环保, 低成本的硒代硫酸钠作为硒源, 制备 In<sub>2</sub>Se<sub>3</sub> 的同时保留了 Sb<sub>2</sub>S<sub>3</sub> 原始的优势取向, 为水热法制备硒化物提供了一种新的思路。

**关键词:** 硫化锑, S 型异质结, 气相输运沉积法, 硒代硫酸钠

#### 参考文献

- [1] Y. Chen, Y. Cheng, J. Zhao et al. *Journal of Colloid and Interface Science* 627 (2022) 1047 - 1060.
- [2] Jin L, Wu Y, Zhang H, et al. *Chemistry - A European Journal*, 2022, 28(14): e202104428.

# Passively Q-switched mode-locking Er-doped fiber laser with tunable wavelength and pulsating soliton

Chenxu Ren, Yu Fang, Baole Lu, Mei Qi, Jintao Bai

No.1 Xuefu Street, Guodu Education Technology Industrial Zone, Chang'an District, Xi'an 710127

**Abstract:** A passively Q-switched mode-locking erbium-doped fiber laser with tunable wavelength and pulsating soliton is demonstrated. The polarization-maintaining erbium-doped fiber, working as the gain medium, combines with nonlinear polarization rotation to form a Lyot filter in the cavity. A tapered fiber is placed between two polarization controllers to cause a significant insertion loss in the optical path, which makes it easy to generate Q-switched mode-locking (QML) pulses. The wavelength tunable QML laser is implemented simply and easily, and the tunable wavelength ranged from 1528.05 nm to 1569.55 nm, as large as 41.5 nm. In addition, a new type of QML pulse involving pulsating soliton has been discovered in the laser, which was called Q-switched harmonic mode-locking pulsating soliton (QHML-PS). We find that the harmonic order and repetition frequency increases with the rising of the pump power. Our work has tremendous significance for expanding the research and application of emerging QML fiber lasers.

**Key Words:** Er-doped fiber, Q-switched mode-locking, Pulsating-soliton

## 铌酸锂波导中宽带二次谐波的产生

全珍珠, 何云东, 管佳豪, 薛少杰, 齐新元\*

西北大学, 西安, 710127

qixycn@nwu.edu.cn

**摘要:** 二阶非线性光学频率转换在光谱学、频率计量学、传感以及光通信等领域都有着重要的应用, 它可以灵活地产生所需波长的相干光, 而激光增益介质不容易获得该相干光。准相位匹配 (QPM) 技术是实现频率转换的一种重要手段, 它通过周期性改变非线性介质的极化方向以提高晶体的非线性频率变换效率; 铌酸锂 (LiNbO<sub>3</sub>) 晶体具有较大的二阶非线性系数 ( $d_{33}=25\text{pm/V}$ )、从紫外到中红外的宽透明范围和高折射率, 是波长转换的合适的  $\times(2)$  材料选择。Miyazawa<sup>[1]</sup> 在 1985 年证实了可以在铌酸锂晶体中实现准相位匹配。目前已有研究表明, 通过 QPM 技术与铌酸锂纳米光子波导相结合, 可实现高效的二次谐波 (SHG), 但存在较窄带宽问题, 仅为几纳米, 在此基础上, 通过设计晶体结构, 如多晶体级联, 啁啾匹配等, 可实现宽带倍频<sup>[2]</sup>, 这在多波长和超短脉冲倍频等领域有着重要应用, 但特殊结构的设计会促使效率的降低, 为了确保高效的二次谐波效率, 可通过热光学提高其波长可调谐性, 最终实现高效率的宽带倍频。通常为了实现高可调谐性, 大多采用了 I 型相位匹配方案, 以利用 LN 中最大的热光双折射系数, 然而, 这种方案的 SHG 效率降低了 30 倍, 0 型准相位匹配方案可以利用  $d_{33}$  实现高效率, 但由于热光系数小得多, 因此可调谐性较低。效率和可调谐性之间的这种失衡对实现由 LN 制成的非线性光学器件的更高性能造成了限制。那么现采用在最小化相互作用波长的群速度失配基础上设计晶体结构来实现宽带倍频, 这不仅使其维持高转换效率, 并且具有可调谐性, 这种技术可用于超短相干光脉冲的频率转换、超连续谱生成、模式选择频率转换和高维量子信息处理。

**关键词:** 准相位匹配; 二次谐波, 宽带能量转换

参考文献

- [1] Thaniyavarn S, Findakly T, Booher D, et al. Domain inversion effects in Ti-LiNbO<sub>3</sub> integrated optical devices[J]. Applied Physics Letters, 1985, 46(10):933-93.
- [2] Chen BQ, Zhang C, Hu CY, Liu RJ, Li ZY. High-Efficiency Broadband High-Harmonic Generation from a Single Quasi-Phase-Matching Nonlinear Crystal. Phys Rev Lett. 2015 Aug 21;115(8):083902.
- [3]

## 基于 NPR 的 C 波段和 L 波段锁模光纤激光器

王毅, 陆宝乐

西北大学 710127 light\_chaser@sohu.com

**摘要:** 工作在 L 波段的超快激光器可以将光通信系统中主要在 C 波段应用的波分复用技术延伸到 L 波段, 进一步提高通信容量, 并在光谱学、生物医学诊断和外科等领域应用广泛。我们搭建了基于非线性偏振旋转 (NPR) 的 C 波段和 L 波段掺铒锁模光纤激光器, 通过调节半波片、四分之一波片和泵浦功率实现了 1567.7 nm 和 1599.3 nm 之间的波长可切换操作。在 1567.7 nm 波段产生束缚态, 信噪比为 80 dB, 基频为

15.77 MHz, 在 1599.3 nm 波段产生传统孤子, 通过调节半波片, 即改变腔内损耗, 实现了束缚态与传统孤子的可切换操作。这种具有 C 波段和 L 波段可切换的超快光纤激光器被认为是一种拥有广泛应用的有效光源。

关键词: 锁模光纤激光器, NPR, 束缚态, L 波段

## 谷光子晶体中的拓扑边界态

万鑫, 温芝希, 何云东, 彭晨阳, 李港, 齐新元\*

西北大学, 西安, 710127

qixycn@nwu.edu.cn

**摘要:** 光子晶体 (Photonic Crystal, PC) 这一概念最初是在 1987 年由 Eli Yablonovitch (美) 和 Sajeev. John (加) 在研究周期性电介材料时分别提出的。其是一种在一维、二维或三维高度有序排列、具有光子带隙的人造周期性电介质结构。PC 不仅将大自然装饰得绚丽多彩, 而且还提供了一种强大的手段来操纵和控制光的传播。光量子谷霍尔效应的实现需引入能谷自由度。在不依赖自旋轨道耦合效应前提下, 通过打破空间反演对称性以实现能谷 (K 与 K' 谷) 附近的能带简并打开, 实现类比电子能谷霍尔效应的光学赝自旋依赖的路径关联传输。现主要存在两种方式引入能谷自由度。一是采用电磁对偶能谷光子晶体, 二是采用全电介质的能谷光子晶体。实现拓扑边界态的方法有很多, 基于物理效应可分为: 量子霍尔效应、Floquet 拓扑绝缘体、量子自旋霍尔效应、量子谷霍尔效应等。基于对称性, 从最初的外加磁场打破时间反演对称性[1], 到构建等效磁场打破时间反演对称性[2], 再到打破空间反演对称性[3]。无论是材料还是研究方法, 拓扑边界态的发展趋势都是采用更易制备的材料, 更易实现的方法, 即简单高效地实现拓扑边界态。光子晶体的光子中经历与晶体中的电子类似的周期性势场, 经过精细设计后可以出现各种能带结构。拓扑光子学的出现与发展为更好地控制调控光子提供了可能, 其产生的拓扑边界态因可实现缺陷免疫、绕障碍物、抗散射的单向传输等优良特性, 而被广泛研究并有待应用于光集成与光通讯领域。谷作为一个重要的自由度被引入光子拓扑相的设计构建中, 由于强大的谷传输不需要磁性材料和复杂的光子赝自旋结构, 因此, 本课题设计了基于六芒星与六边形的 C3 对称的谷光子晶体, 通过采用降低晶格对称性的方法打破系统的空间反演对称性, 简并的狄拉克点退化, 出现了带隙。能谷边界态出现在拓扑性质不同的光子晶体结构的畴壁。拓扑光波导可以由两种具有不同拓扑性质的能谷光子晶体构建, 光在波导上传输时会被局域在交界面上, 表现出能谷光子晶体的奇异传输性质: 拓扑能谷运输。在 U 型波导中验证了边界态的鲁棒性, 其遇到转角仍有抗散射能力。

### 参考文献

- [1] Ling Lu, Chen Fang, Liang Fu, et al. Symmetry-protected topological photonic crystal in three dimensions. *Nature Phys* 12, 337–340 (2016).
- [2] Kejie Fang, Zongfu Yu, and Shanhui Fan. "Photonic Aharonov-Bohm Effect Based on Dynamic Modulation." *Physical Review Letters* 108, 15, 153901 (2012).
- [3] Yuting Yang, Hua Jiang & Zhi Hong Hang. Topological Valley Transport in Two-dimensional Honeycomb Photonic Crystals. *Sci Rep* 8, 1588 (2018).

## A high stability and low noise passively Q-switched yellow-green laser at 561 nm with a Ti3C2Tx-PVA saturable absorber

Guozhen Wang<sup>1</sup>, Yang Bai<sup>1, 2</sup>, Ben Li<sup>1</sup>

1. Institute of Photonics & Photon-Technology, Northwest University, Xi'an 710127, China

2. Shaanxi Engineering Technology Research Center for Solid State Lasers and Application, Xi'an 710127, China

**Abstract:** Using a Ti3C2Tx-polyvinyl alcohol (PVA) film SA, a Brewster polarizer (BP), a birefringent crystal (BC), and a type-I critical phase-matched crystal LBO, a 561 nm passively Q-switched yellow-green (PQYG) laser with high power stability and low noise was faultlessly realized based on an 808 nm LD end-pumped Nd: YAG ceramic and intracavity frequency doubling. BP and BC effectively suppressed the oscillation of the 1112 nm and 1116 nm spectral lights in the cavity and reduced the number of longitudinal modes of the 1123 nm fundamental frequency light. At 5.11 W of LD pump power, the 561 nm PQYG laser with a 75.5 mW average output power, 609.8 kHz repetition rate, and 41 ns pulse width were obtained, corresponding to a low power instability of  $\pm 0.21\%$  and a low laser noise of 0.49%. The results demonstrate that the

"Ti<sub>3</sub>C<sub>2</sub>T<sub>x</sub>-PVA film passive Q-switching + BP-frequency selection + BC-filtering" technology path provides a valuable reference for developing pulsed laser with high stability and low noise.

**Keywords:** Passively Q-switched; Ti<sub>3</sub>C<sub>2</sub>T<sub>x</sub>-PVA film; 561 nm yellow-green laser; High stability; Low noise

This work investigates a 561 nm passively Q-switched yellow-green (PQYG) laser based on 808 nm LD end-pumped Nd: YAG ceramic, Ti<sub>3</sub>C<sub>2</sub>T<sub>x</sub>-PVA film passive Q-switching, and LBO crystal intracavity frequency doubling. In the cavity, a Ti<sub>3</sub>C<sub>2</sub>T<sub>x</sub>-PVA film with a thickness of 14.1 μm, a saturation light intensity of 2.08 MW/cm<sup>2</sup>, and a modulation depth of 5.18% was used as a saturable absorber for generating pulse lasers. The frequency selection function of a Brewster polarizer (BP) effectively suppressed the intracavity oscillation of spectral light at 1112 nm and 1116 nm, ensuring that only 1123 nm fundamental frequency light oscillated in the cavity. The filtering function of a birefringent crystal (BC) further compressed the number of longitudinal modes at 1123 nm. All these were beneficial to improve the power stability of the 561 nm PQYG laser and reduce its laser noise. Using a type-I critical phase-matched frequency doubling crystal LBO in the cavity, the 561 nm PQYG laser with a 75.5 mW average output power, 609.8 kHz repetition rate, and 41 ns pulse width were obtained at 5.11 W of LD pump power, corresponding to a ±0.21% low power instability and a 0.49% low laser noise. The results demonstrate that the "Ti<sub>3</sub>C<sub>2</sub>T<sub>x</sub>-PVA film passive Q-switching + BP-frequency selection + BC-filtering" technology path provides a valuable reference for the development of pulsed 561 nm yellow-green laser with high power stability and low noise.

References

### 基于GO-COOH 可饱和吸收体的 1 μm 锁模光纤激光器

严义, 陆宝乐, 白晋涛西北大学 710127 [522322159@qq.com](mailto:522322159@qq.com)

**摘要:**二维材料具有低损耗、超快载流子响应以及宽波段的非线性吸收等特性, 被广泛应用于产生超短脉冲激光。羧基氧化石墨烯(GO-COOH)材料因其良好的水溶解度, 极大降低了制备难度以及制造成本, 更适合制备具有高调制深度以及低非饱和损耗的可饱和吸收体。目前, GO-COOH 作为可饱和吸收体已在 1.5 μm 波段获得了锁模脉冲, 但在 1 μm 波段仅报道过结合非线性偏振旋转与GO-COOH 可饱和吸收体的混合锁模脉冲输出。本文搭建了基于 GO-COOH 可饱和吸收体的掺镱脉冲光纤激光器, 获得了中心波长为 1060.74 nm, 重复频率为 23.32 MHz, 信噪比为 68.49 dB 的锁模脉冲。

**关键词:**锁模光纤激光器, GO-COOH, 耗散孤子, 1 μm

### The construction of Bi<sub>2</sub>O<sub>2</sub>S/ZnIn<sub>2</sub>S<sub>4</sub> 2D heterojunction by cascade electric field with enhanced photoelectrochemical properties

Xueling Wei, Xiaoyun Hu, Hui Miao\*

School of Physics, Northwest University, Xi'an, Shaanxi 710127, PR China

\*E-mail: huim@nwu.edu.cn

**Abstract:** Photoelectrocatalytic water splitting technology is an effective way to convert solar energy into hydrogen energy to obtain clean energy. Bi<sub>2</sub>O<sub>2</sub>S has promising photoelectric properties, such as narrow bandgap (1.13–1.5 eV), strong light absorption, excellent electrical transmission performance, and non-toxicity [1]. Because of that, it is widely used in optoelectronic devices as an n-type semiconductor. In this work, ultra-thin Bi<sub>2</sub>O<sub>2</sub>S nanosheets were synthesized on FTO glass substrate using a simple one-step hydrothermal method. Firstly, in order to solve the problems of weak connection interfaces and poor charge transfer efficiency in traditional heterojunction composites, this work adopts an in-situ growth method to construct a Bi<sub>2</sub>O<sub>2</sub>S/ZnIn<sub>2</sub>S<sub>4</sub> nanosheet heterojunction with super strong inter plane interactions and high internal electric field, which allows photogenerated holes to quickly migrate to the surface of Bi<sub>2</sub>O<sub>2</sub>S and participate in oxygen evolution reactions, further suppressing the recombination

of photogenerated electron hole pairs. Secondly, ZnIn<sub>2</sub>S<sub>4</sub> with [S-In]-[S-In-S]-[Zn-S] asymmetric layered structural units have asymmetric polarization of the crystal, which is beneficial to overcome the problem of slow hole transport in the oxidation reaction [2]. The prepared samples were characterized by X-ray diffraction (XRD), scanning electron microscopy (SEM), UV-vis-NIR diffuse reflectance spectra, and photoelectrochemical testing. Compared with pure Bi<sub>2</sub>O<sub>2</sub>S photoelectrode, the Bi<sub>2</sub>O<sub>2</sub>S/ZnIn<sub>2</sub>S<sub>4</sub> photoelectrode exhibits superior photoelectrochemical properties. Under the conditions of 1.23 V vs. RHE, the photocurrent density of the composite material reached 4.821 mA/cm<sup>2</sup>, which is eight times that of Bi<sub>2</sub>O<sub>2</sub>S. Electrochemical impedance spectroscopy (EIS) testing shows that ZnIn<sub>2</sub>S<sub>4</sub> can effectively enhance the interfacial charge transfer kinetics of Bi<sub>2</sub>O<sub>2</sub>S, enabling faster migration of photogenerated electrons at the interface. According to SEM, the introduction of ZIS nanosheets makes Bi<sub>2</sub>O<sub>2</sub>S nanosheets rougher, which increases the active sites on the surface of Bi<sub>2</sub>O<sub>2</sub>S and further enhances its oxygen evolution reaction (OER) activity. This study provides new insights for the design of Bi<sub>2</sub>O<sub>2</sub>S based photoelectrodes.

**KeyWords:** Bi<sub>2</sub>O<sub>2</sub>S, Cascade electric fields, Charge separation, Nanosheet, Photoelectrochemical

- References
- [1] J. Huang, Z.R. Xie, J.X. Chen, et al., *J. Lumin.*, 263, 120004 (2023).
  - [2] J. Wan, L. Liu, Y. Wu, et al., *Adv. Funct. Mater.*, 32(35), 2203252 (2022).

### Stable single longitudinal mode ytterbium-doped fiber laser with ultra-narrow linewidth and high OSNR using a double-ring passive subcavity

Han Wen<sup>1,2</sup>, Yaqi Zhai<sup>1,2</sup>, Baole Lu<sup>1,2</sup> and Haowei Chen<sup>1,2\*</sup>

1. State Key Laboratory of Energy Photon-Technology in Western China, International Collaborative Center on Photoelectric Technology and Nano Functional Materials, Institute of Photonics & Photon-Technology, Northwest University, Xi'an 710127, China
2. Shaanxi Engineering Technology Research Center for Solid State Lasers and Application, Shaanxi Provincial Key Laboratory of Photo-Electronic Technology, Northwest University, Xi'an 710127, China

\* Correspondence: [chenhaowei0320@163.com](mailto:chenhaowei0320@163.com)

**Abstract:** A continuous wave (CW) ultra-narrow linewidth single-longitudinal mode (SLM) ytterbium-doped fiber laser (YDFL) based on narrowband fiber Bragg grating (NB-FBG) and double-ring passive subcavity (DR-PS) was studied. The filtering characteristics of the double-ring passive subcavity are analyzed theoretically, and it is used as a high-precision mode filter to eliminate the dense longitudinal mode and mode hopping of YDFL and ensure that the laser operates in the SLM state. Experimental results show that the laser has a central wavelength of 1030.052 nm at room temperature, an optical signal-to-noise ratio of up to 73 dB, and an ultra-narrow linewidth of 355 Hz. In addition, we measured the short-term and long-term stability of the laser, with wavelength and power fluctuations of less than 0.008 nm and 0.19 dB, respectively, over 120 min. As a result, we obtain SLM YDFL with high stability, ultra-narrow linewidth, and a high optical signal-to-noise ratio.

### 激光参数对石材涂层脉冲激光清洗的影响

徐知微

西北大学光子学与光子技术研究所, 西安 710127

2895068186@qq.com

**摘要:** 为了有效去除汉白玉表面油漆, 采用面积外推法和激光诱导等离子体光谱法(LIPS)获得了金、银涂层和汉白玉表面的烧蚀阈值功率。在此基础上, 确定在不损坏汉白玉基底的情况下去除油漆的最佳激光功率。利用图像处理技术, 研究了激光清洗 10mm×10mm 汉白玉表面金银漆的清洗程度和清洗率的变化趋势。获得了最佳激光光斑重叠率和最佳清洗时间。最后, 利用图像处理对激光清洗汉白玉表面油漆层的清洗效果进行了评价。93%以上的清洁度表明, 面积外推法、LIPS 法和图像处理法的协同使用可以有效提

高汉白玉表面涂层的激光清洁效率。

关键词：激光清洗；白色大理石；金色油漆；银色油漆；LIPS 法；图像法

通过开展基于面积外推法的汉白玉基材表面金色、银色两种油漆层的激光烧斑面积随激光功率的变化规律研究、汉白玉基材表面 LIPS 光谱峰值随激光功率的变化规律研究和基于图像法的油漆层表面焦状物占比随激光功率的变化规律研究，确定了 100 kHz、200 ns 固定激光参数下汉白玉表面金色、银色两种油漆层的最佳激光功率为 40 W；利用图像法研究了 20 mm × 20 mm 区域内金色、银色两种油漆层的清洗度随光斑搭接率变化的规律，结合求解清洗速率，确定了最佳光斑搭接率分别为 10%和 30%，对应最少清洗次数分别为 5 次和 4 次。在固定参数和最佳参数 条件下，实现了清洗度分别达到 95.93%和93.89%的汉白玉表面金色油漆、银色油漆的高质量清洗。

## 10kW 矩形光斑空间非相干合束器设计

闫佳乐

西北大学 光子学与光子技术研究所，西安 710127

675762087@qq.com

摘要:本文按照矩阵平行排列 18 束光纤输出的 972 nm 半导体激光束，通过光束准直和空间非相干合束，获得了具有矩形光斑特征的 10 kW 级合束激光。在理论分析准直激光束的半径、相邻光束间距与合束激光的光斑搭接率之间变化规律的基础上，利用光学设计软件建立起合束器结构模型并模拟出合束激光光斑能量分布，完成 10 kW 级 18 ×1 的矩形光斑激光合束器的研制。在 200 mm 的合束长度内实现了具有单一矩形光斑形貌、最大合束功率 10.249 kW、焦斑尺寸 31 mm × 11 mm、中心波长 972.34 nm、谱线宽度 2.27 nm 的合束激光输出。关键词:非相干空间合束，光学设计，矩形光斑随着工业大功率激光器及其辅助设备的实用化，先进激光技术与各类大型设备的零部件表面强化与改性技术升级紧密地结合在一起。其中，激光金属材料表面热处理技术作为金属材料表面强化和改性最有效的手段之一，成为了国内外研究的热点。光纤传输横截面为矩形的激光光束不仅可以有效提高激光热处理的效率，而且能够在狭小的零部件内部实施柔性激光热处理。基于激光非相干空间合束原理并结合光学设计及仿真，研制出一款连接 18 台 972 nm 光纤输出半导体激光器的 18×1 矩形光斑激光非相干空间合束器，实验获得了在 200 mm 合束长度内具有单一矩形光斑特征、10.249 kW 最大合束功率、98.5% 合束效率的空间非相干合束激光。合束激光的中心波长为 972.34 nm、谱线宽度为 2.27 nm、焦斑尺寸为 31 mm×11 mm、功率不稳定性小于±1.2%。

## Influence of laser parameters on corrosion resistance of laser melting layer on C45E4 steel surface

Jingyan Yang<sup>1</sup>, Yang Bai<sup>1,2,3,4</sup>, Tianxuan Bian<sup>1,2</sup>, Zhiwei Xu<sup>1,3,4</sup>

1. Institute of Photonics & Photon-Technology, Northwest University, Xi'an, Shaanxi 710127, China
2. State Key Laboratory of Photon-Technology in Western China Energy, Xi'an, Shaanxi 710127, China
3. Shaanxi Engineering Technology Research Center for Solid State Lasers and Application, Xi'an, Shaanxi 710127, China
4. Key Laboratory of Metrological Optics and Application for State Market Regulation, Shaanxi Institute of Metrology Science, Xi'an, Shaanxi 710199, China  
jy2428337125@163.com

**Abstract:** C45E4 steel is one of the medium carbon steels widely used in mechanical engineering. However, every year, industries pour huge human and financial resources into repairing or replacing the functionally C45E4 steel parts that are exposed to corrosion environment. In this paper, a single factor laser melting experiment on C45E4 steel surface by using a pulsed laser beam at a wavelength of 1064 nm and electrochemical analysis found the optimal laser parameter combination: single-pulse energy density of 3.82 J·cm<sup>-2</sup>, spot overlap rate of 80% and 4 number of laser scans. The thickness of the optimal laser melting layer prepared with the optimal laser parameters was only 10.85 μm, and it had a maximum self-corrosion potential of 1.031 V, a minimum corrosion current of 3.451 × 10<sup>-9</sup>A·cm<sup>-2</sup> and a maximum charge transfer resistance of 1541.2 Ω·cm<sup>-2</sup>. The optimal laser melting layer had a stable Fe<sub>3</sub>O<sub>4</sub>-FeO corrosion resistance structure, effectively reduced the surface roughness, microcrack density and oxidation leakage point, and prevented the C45E4 steel surface from being over-oxidized.

**KeyWords:** Laser melting, C45E4 steel, Optimal laser parameters, Corrosion

resistance, Electrochemistry

In summary, a series of laser melting layers with corrosion resistance are prepared on the medium carbon steel C45E4 by using a pulsed laser. Through EIS, SEM, surface roughness, EDS and XRD analysis, the influence of laser parameters including the single-pulse energy density, spot overlap rate and laser scanning times on the corrosion resistance of the laser melting layers are studied. It was found that single pulse energy density, spot overlap rate, and laser scanning have significant effects on the distribution of microcracks, self-corrosion potential, and unit corrosion current of the laser melting layer. The optimal laser parameters is determined and the optimal laser melting layer with high corrosion resistance is prepared. The 10  $\mu\text{m}$ -thick optimal laser melting layer is prepared on 2.5 mm-thick C45E4 steel plate at the optimal laser parameters. Specifically, the optimal single-pulse energy density is  $3.82 \text{ J}\cdot\text{cm}^{-2}$ , the optimal spot overlap rate is 80 % and the optimal number of laser scans is 4. The corrosion resistance of the optimal laser melting layer is increased by 3 times, compared with that of the hot alkaline blackening layer with the same thickness prepared by the traditional process.

### 非互易厄米沙漏光子晶格能带调控及其光传输的影响

杨俊豪<sup>1</sup>, 王元旦<sup>2</sup>, 齐新元<sup>1\*</sup>西北大学, 西安, 710127

qixycn@nwu.edu.cn

摘要: 平带光子晶格结构, 由于其能谱中至少存在一个完全无色散的能带, 进而可获得对缺陷、无序等免疫的紧凑局域模, 因此受到广泛关注。但就目前而言, 绝大多数平带光子晶格结构的临近波导耦合都是互易耦合作用, 且一种结构只能获得单一的功能。受此启发, 我们设计了一个非对称体系, 既能实现平带也能实现能带的调控, 且功能多样。结果表明: 在非互易耦合系数的作用下此光子晶格不仅能产生两种平带结构, 还存在能带反转现象。进一步研究表明, 此结构可实现光隔离现象, 并具有多种不同的光传输现象, 例如分叉光。且这些传输现象和能带相关。在平带条件下具有非对称局域传输以及无衍射传输。此外, 在系统存在缺陷时, 此系统具有特殊的双边界态。我们的研究可推动了人工光子晶格能带调节理论的发展。

关键词: 非互易, 平带; 能带反转; 分叉光; 双边界态

支持信息: 国家自然科学基金 (1217040857)。

### Defects regulation of $\text{Sb}_2(\text{S}, \text{Se})_3$ by construction of $\text{Sb}_2(\text{S}, \text{Se})_3/\text{CdSe}$ direct S-scheme heterojunction with enhanced photoelectrochemical performance

Yuanhao Yanga, Xiaoyun Hua, Hui Miao<sup>\*</sup>

School of Physics, Northwest University, Xi'an, Shaanxi 710127, PR China

\*E-mail: huim@nwu.wdu.cn

**Abstract:** Photoelectrochemical (PEC) water splitting technology is expected to promote the reform of global energy distribution and accelerate the realization of the “two-carbon goal” [1]. Of particular note, as a novel photoelectrochemical material,  $\text{Sb}_2(\text{S}, \text{Se})_3$  is identified as a promising light-harvesting material due to its excellent light-harvesting capability, abundant elemental storage. However,  $\text{Sb}_2(\text{S}, \text{Se})_3$  has a large number of defective energy levels, which limits its application in the PEC field. Cadmium selenide (CdSe) film is one promising II-VI semiconductor compound with a direct optical band gap. CdSe is an attractive compound due to its small size and its large absorbance in the visible light spectrum, originating from quantum confinement effect and large surface to volume ratio [2]. Most of the existing methods for preparing CdSe include reducing Se powder with toxic substances such as hydrazine hydrate, acetone, and ammonia. In this work, we successfully prepared CdSe thin films and constructed  $\text{Sb}_2(\text{S}, \text{Se})_3/\text{CdSe}$  S-type heterojunctions using a cheap, environmentally, friendly, and non-toxic Se precursor solution to effectively eliminate the adverse effects of  $\text{Sb}_2(\text{S}, \text{Se})_3$  defect levels.  $\text{Sb}_2(\text{S}, \text{Se})_3$  thin films and  $\text{Sb}_2(\text{S}, \text{Se})_3/\text{CdSe}$  S-scheme heterojunctions were prepared on ITO substrates by hydrothermal methods. The S-scheme



heterojunction formed by  $\text{Sb}_2(\text{S},\text{Se})_3$  and CdSe provided a stronger driving force to optimize carrier interface transportation. The CdSe nanoparticles grown in situ on  $\text{Sb}_2(\text{S},\text{Se})_3$  thin films significantly reduce the recombination loss of photogenerated electron hole pairs, significantly increase the carriers lifetime, and enhance the oxidation ability of the photoelectrode. The photocurrent density was  $1.71 \text{ mA/cm}^2$  at  $1.23 \text{ V vs. RHE}$ , which was 14.2 times higher than pure  $\text{Sb}_2(\text{S},\text{Se})_3$  ( $0.12 \text{ mA/cm}^2$ ). The  $\text{Sb}_2(\text{S},\text{Se})_3/\text{CdSe}$  S-type heterojunction reduces electron transfer resistance, enhances light absorption ability, and increases surface active sites, thus greatly improving the PEC ability. This work opens up a new way for the design of  $\text{Sb}_2(\text{S},\text{Se})_3$  photoelectrodes.

**Keywords:**  $\text{Sb}_2(\text{S},\text{Se})_3$ , CdSe, direct S-scheme heterojunction, defects regulation, photoelectrochemical performance

### 基于NALM 锁模的光纤激光器研究

杨雪育

西北大学 710127

[xueyuyang3@163.com](mailto:xueyuyang3@163.com)

摘要:我们搭建了基于非线性放大环镜(NALM)锁模的全正态色散(ANDi)掺镱(Yb)光纤激光器,该激光器不仅允许可调谐的单波长和类噪声输出而且能够产生不同孤子类型的双波长。单波长调谐范围为  $1028.51 \text{ nm}$ - $1078.69 \text{ nm}$ , 共  $50.18 \text{ nm}$  的调谐量。类噪声的调谐范围为  $1035.14 \text{ nm}$ - $1069.05 \text{ nm}$ , 尖峰脉宽在  $543 \text{ fs}$ - $755 \text{ fs}$  变化。在  $1031.37 \text{ nm}/1043.76 \text{ nm}$ ,  $1038.71 \text{ nm}/1051.66 \text{ nm}$ ,  $1037.38 \text{ nm}/1061.46 \text{ nm}$  能够实现双波长输出, 这些双波长间隔是不等的。同时, 在  $1033.79 \text{ nm}/1039.17 \text{ nm}$  实现了耗散孤子和类噪声共存的双波长输出, 其对应的重频差为  $1037 \text{ Hz}$ 。我们的实验结果有助于对不同孤子类型输出光纤激光器的研究, 并为掺镱双梳源提供了一种新思路。

关键词:锁模光纤激光器, 非线性放大环境, 耗散孤子, 类噪声

### 基于Nd/Yb 近红外双模光学温度传感探针的研究

李丹

西安邮电大学, 西安 710121

[1758484280@qq.com](mailto:1758484280@qq.com)

摘要:温度传感器是指感受温度并输出信号的传感器。在光热治疗中, 温度的准确性至关重要, 本文主要利用光与温度的关系制作可以获取生物体内组织温度, 达到非接触式测温的目的。近年来, 和可见光和紫外光相比, 近红外光因其穿透力强, 散射和透射光较少, 具有较大的优势。近红外发光纳米测温方法非常适合于生物组织体内的温度检测。本文采用热分解法制备了六方相  $\text{NaYF}_4:\text{Nd}_{0.015}/\text{Yb}_{0.1}/\text{Gd}_x/\text{NaNdF}_4$  ( $x=0, 0.5, 0.885$ ) 纳米晶体。制备双模近红外光温度探针。其中样品的 XRD 和 TEM 数据表明, 样品具有良好的分散性。掺杂了  $\text{Gd}^{3+}$  使样品  $\text{NaYF}_4:\text{Nd}/\text{Yb}$  的  $850\text{-}950\text{nm}$  处发光强度增强。外面又包覆一层惰性壳增加了  $975\text{nm}$  和  $1055\text{nm}$  处的强度。由于发光依赖于温度, 故以不同的发光强度峰值为中心的积分强度比作为两个温度传感器。此外, 基于 LIR 技术, 在  $808\text{nm}$  激光激发下, 研究了两个传感器的温度传感性能。结果表明, 样品在生物组织的温度传感方面具有潜在的应用前景。

关键词:稀土发光, 温度传感, 近红外发射, 双模测温

### 基于SSA-LSTM 方法的被动锁模光纤激光器脉冲特性沿腔内位置演化预测研究

张博媛, 郭若彤, 陈雅妮, 韩冬冬\*

西安邮电大学, 电子工程学院, 710121

\* [handongdong@xupt.edu.cn](mailto:handongdong@xupt.edu.cn)

摘要:在被动锁模光纤激光器系统中, 超短脉冲沿腔内位置的演变是一个极其复杂的计算过程。在此, 我们提出了一种数据驱动模型, 利用麻雀搜索算法(SSA)和长短期记忆(LSTM)方法相结合, 预测脉冲特性沿腔内位置的复杂腔内演化过程, 而不是数值计算非线性薛定谔方程(NLSE)。此外, 还将提出的SSA-

LSTM 模型与单独的LSTM 网络进行了比较。神经网络预测的结果与NLSE 模拟的结果非常吻合，并且SSA-LSTM 模型还表现出卓越的预测性能。

关键词:被动锁模光纤激光器, 腔内演化, 长短期记忆神经网络, 麻雀搜索算法

### Predicting evolutions of pulse characteristics along cavity position in passively mode-locked fiber laser via SSA-LSTM approach

*Boyuan Zhang, Ruotong Guo, Yani Chen and Dongdong Han\**

School of Electronic Engineering, Xi'an University of Posts and Telecommunications, Xi'an 710121, China

**Abstract:** Ultrashort pulse evolution along the cavity position is an extremely complicated computational process in passively mode-locked fiber laser systems. Herein, we present a data-driven model to predict the complex intracavity evolution of pulse characteristics along the cavity position using an integrated sparrow search algorithm (SSA) and long short-term memory (LSTM) approach instead of numerically calculating the nonlinear Schrödinger equation (NLSE). Furthermore, the proposed model is compared with a separate LSTM network. The results predicted from the network agree well with those of the NLSE simulation. Moreover, the SSA-LSTM model exhibits excellent predictive performance.

**Keywords:** Passively mode-locked fiber laser, Intracavity evolutions, Long short-term memory network, Sparrow search algorithm

### Bi2O2S topological transformation and in-situ regrowth of [hk1]-oriented SbBiS3-xSex 2D skeleton structure for construction of efficient quasi-two-dimensional Sb2S3-xSex-based heterojunction photoanodes

*Liyuan Zhanga, Xiaoyun Hua, Hui Miao<sup>a,\*</sup>*

School of Physics, Northwest University, Xi'an, Shaanxi 710127, PR China

\*E-mail: huim@nwu.wdu.cn

**Abstract:** Antimony chalcogenides ( $\text{Sb}_2\text{S}_3-x\text{Se}_x$ ), as one of the promising light-absorbing materials in optoelectronic energy storage devices, has attracted widespread attention in recent years<sup>[1]</sup>. Of particular note, its crystal structure consists of the one-dimensional  $[\text{Sb}_4\text{S}(\text{Se})_6]_n$  ribbons with efficient carrier transport efficiency along the [hk1] direction<sup>[2]</sup>. The open frame structure of Bi<sub>2</sub>O<sub>2</sub>S will form an internal electrostatic field between the layers, which has a good promotion effect on the transport and separation of photogenerated carriers. In this work, we used Bi<sub>2</sub>O<sub>2</sub>S as a template to induced growth through topological transformation and cleverly introduced Bi elements to synthesize SbBiS<sub>3-x</sub>Se<sub>x</sub> bimetallic alloy and the conversion of Sb<sub>2</sub>S<sub>3-x</sub>Se<sub>x</sub> preferred orientation from [hk0] to [hk1] was realized. Certain morphological characteristics of Bi<sub>2</sub>O<sub>2</sub>S were reprinted, resulting in a 2D skeleton structure that was conducive to the construction of light trap. The interface charge transfer resistance was reduced and the electrochemically active surface area was increased. At the same time, Bi<sub>2</sub>O<sub>2</sub>S was employed as the transport layer to achieve rapid conduction of electrons. Finally, Bi<sub>2</sub>O<sub>2</sub>S and introduced Bi elements worked synergistically to greatly improve the PEC performance of Sb<sub>2</sub>S<sub>3-x</sub>Se<sub>x</sub> photoelectrode. When the applied bias voltage was 1.23 V vs. RHE, the photocurrent density of the prepared Bi<sub>2</sub>O<sub>2</sub>S/SbBiS<sub>3-x</sub>Se<sub>x</sub> photoanode reached 6.41 mA cm<sup>-2</sup>, which was 7.5 times (0.86 mA cm<sup>-2</sup>) of the pure Sb<sub>2</sub>S<sub>3-x</sub>Se<sub>x</sub> photoelectrode. The onset potential displayed a significant negative shifted, and the value of IPCE was as high as 40.93%. In addition, combined with related characterization, it was confirmed that the underlying interface engineering of Bi<sub>2</sub>O<sub>2</sub>S played an important role in improving the catalytic performance of Sb<sub>2</sub>S<sub>3-x</sub>Se<sub>x</sub> photoanode, and the growth mechanism of SbBiS<sub>3-x</sub>Se<sub>x</sub> bimetallic alloy with 2D skeleton structure (nanoneedles interwoven nanosheets) was given. This study provided new insights for modifying Sb<sub>2</sub>S<sub>3-x</sub>Se<sub>x</sub> through the underlying interface to obtain a promising PEC water splitting photoanodes.

**Keywords:** quasi-two-dimensional heterojunction;  $\text{SbBiS}_{3-x}\text{Se}_x$ ; 2D skeleton structure;  $\text{Bi}_2\text{O}_2\text{S}$ ; [hk1] preferred orientation; photoelectrochemical performance

Reference

- [1] B. Che, Z. Cai, P. Xiao, et al., *Adv. Mater.*, 35(6), 2208564, (2022).  
[2] Y. Lu, K. Li, X. Yang, et al., *ACS Appl. Mater. Interfaces*, 13(39), 46858–46865, (2021).

**In-situ construction of 2D/1D  $\text{Bi}_2\text{O}_2\text{S}/\text{Bi}_2\text{S}_3$  heterojunction from the topotactic transformation of  $\text{Bi}_2\text{O}_2\text{S}$  with significantly enhanced photoelectrochemical performance**

*Wenjing Zhang, Xiaoyun Hu, Hui Miao\**

School of Physics, Northwest University, Xi'an, Shaanxi 710127, P. R. China E-mail address: huim@nwu.edu.cn (H. Miao)

**Abstract:** The emerging two-dimensional layered material  $\text{Bi}_2\text{O}_2\text{S}$  has gradually attracted the interest of researchers due to its high carrier mobility, excellent light absorption characteristic and good stability. However, its application in photoelectrochemical water splitting is very limited. In this work,  $\text{Bi}_2\text{O}_2\text{S}$  nanosheets films were prepared on FTO substrates by one-step hydrothermal method, which broke the traditional powder state of  $\text{Bi}_2\text{O}_2\text{S}$  prepared.  $\text{Bi}_2\text{S}_3$ , which belongs to the same orthorhombic crystal system as  $\text{Bi}_2\text{O}_2\text{S}$ , is also a layered material and shares common cations. This structural similarity gives them a high lattice matching degree and the possibility of mutual conversion. Based on this, we achieved topological transformation of  $\text{Bi}_2\text{O}_2\text{S}$  under high temperature and pressure conditions and in situ evolved  $\text{Bi}_2\text{S}_3$  nanowires, synthesizing heterojunction with atomic-level contact interface. The test results indicated that the  $\text{Bi}_2\text{O}_2\text{S}/\text{Bi}_2\text{S}_3$  photoelectrode exhibited extremely high photoelectrocatalytic performance. At 1.23 V vs. RHE, the photocurrent density of the  $\text{Bi}_2\text{O}_2\text{S}/\text{Bi}_2\text{S}_3$  photoelectrode reached  $3.82 \text{ mA}/\text{cm}^2$ , which was 14 times higher than that of monomer  $\text{Bi}_2\text{O}_2\text{S}$  ( $0.27 \text{ mA}/\text{cm}^2$ ), and had good stability within 1 h. In addition, the incident photon to current conversion efficiency and separation efficiency were increased by 15 and 6 times, respectively. The results have shown that  $\text{Bi}_2\text{O}_2\text{S}$  and  $\text{Bi}_2\text{S}_3$  co-shared by Bi atoms promoted atomic-level close contact and stability of the interface, and this high-quality connected heterostructure effectively stimulated the spatial separation of carriers at the interface. In addition, by changing the sulfur source to regulate the nanowire-like  $\text{Bi}_2\text{S}_3$ , the fast transport channel constructed using its anisotropy promoted the transfer of carriers. In coordination with each other, the 2D/1D  $\text{Bi}_2\text{O}_2\text{S}/\text{Bi}_2\text{S}_3$  heterojunction exhibited significantly enhanced PEC performance. Therefore, we believe that this study provides reference and inspiration for the preparation of highly active heterostructures, and expands new paths for the design and application of  $\text{Bi}_2\text{O}_2\text{S}$  based photoelectrodes.

**Keywords:**  $\text{Bi}_2\text{O}_2\text{S}$ , topotactic transformation, atomic-level contact, photoelectrochemical performance

- References  
[1] Z. Wu, H. Yu, S. Shi, et al., *J. Mater. Chem. A*, 7(24), 14776–14789 (2019).  
[2] B. Chitara, T.B. Limbu, J.D. Orlando, et al., *Nanoscale*, 12(30) 16285–16291 (2020).

## The interaction mechanism between Docetaxel and ctDNA based on the Laser Confocal Raman Spectroscopy

*Suli Zhou, Xiaoqiang Feng, Kaige Wang\**

State Key Laboratory of Cultivation Base for Photoelectric Technology and Functional Materials; National Center for International Research of Photoelectric Technology & Nano-Functional Materials and Application; Key Laboratory of Photoelectronic Technology of Shaanxi Province; Institute of Photonics and Photon-Technology, Northwest University, Xi'an 710127, China

**Abstract:** The mechanism of the interaction between docetaxel (DOC) and calf thymus DNA (ctDNA) was investigated with UV-vis spectroscopy, laser confocal Raman spectroscopy and molecular docking method. In the UV-vis spectroscopy experiments, the effects of pH, ctDNA solution concentration, temperature, interaction time, and  $\text{Na}^+$  ions are systematically investigated. The experimental results showed that with the increase of pH, the peak intensity around 200 nm decreased and red shifted, while the peak at 230nm did not change significantly. With more ctDNA molecules added to the mixed solution, there was a subtractive effect but no significant blue shift or red shift, suggesting that the mode of action of ctDNA might be non-classical intercalated binding. The absorption spectrum of DNA-DOC did not show significant changes at different times, indicating the composite has good stability. And the absorbance of DNA-DOC slowly decreases at 230nm as the concentration of NaCl increases, indicating the DOC is electrostatically bound to DNA. In addition, the changes in Raman characteristic peaks indicated that DOC can interact with both the phosphate backbone and the bases of ctDNA molecules. Finally, the molecular docking simulation results were consistent with the experimental results mentioned above. These results are of great significance for the development and research of new anticancer drugs.

**Key Words:** Docetaxel, CtDNA, Interaction Mechanism, Raman Spectroscopy

西安市激光红外学会

地 址:陕西省西安市长安区学府大道 1 号西北大学物理大楼 618 室

邮 箱:[xasli@foxmail.com](mailto:xasli@foxmail.com)

网 站:[www.xasli.org](http://www.xasli.org) QQ 群:201427822

微信公众号:西安市激光红外学会



西安市激光红外学会  
扫一扫二维码，加入群聊。

## 陕西省计量科学研究院简介

陕西省计量科学研究院始建于1958年，是陕西省人民政府计量行政部门依法设置的法定计量检定机构，是西北国家计量测试中心的技术实体，隶属陕西省市场监督管理局，属公益型全额拨款事业单位。

单位地址位于西安市航天基地神舟六路南段580号，占地104亩。现有职工375人，国家一级注册计量师90人，二级注册计量师188人。设置行政、技术管理部门9个，计量研究所8个。经相关部门考核授权建立了国家过程仪表质量检验检测中心（陕西），国家半导体照明产品质量检验检测中心（陕西）；陕西省眼镜产品质量监督检验站等5个省级质检站/中心。获批筹建“一带一路'国家计量测试研究中心（陕西）”，国家市场监管重点实验室（计量光学及应用），开展前瞻性及应用基础研究、重大关键技术及相关公益性技术研究，提升科技创新能力。

负责研究、建立和保存部分国家计量工作基准、西北地区和陕西省最高社会公用计量标准，已建立375项计量标准，包含4项工作基准；取得中国合格评定国家认可委员会《实验室认可证书》，授权360项校准项目。取得国家级检验检测机构《资质认定证书》，检测能力覆盖131个产品1617个参数；授权取得省级检验检测能力93个产品919个参数，居于同类大区计量机构中等偏上水平。

承担西北地区量值传递和量值溯源，保证各种计量器具量值统一、准确一致；承担陕西省计量器具的强制检定工作；接受政府主管部门和国内外有关机构、客户的委托，开展计量器具新产品、进口计量器具的定型鉴定和样机试验、计量校准、公正计量等工作；承担国家和陕西省部分产品的质量监督和委托检验任务，开展计量技术咨询、技术服务等工作，为市场监督管理提供技术保证。

## 企业简介

Introduction

北京茂丰光电科技有限公司成立于2010年1月，公司成立至今，我们一直秉承“创新和突破”的研发理念，秉承“全心全意为客户”的服务宗旨，秉承“努力实现进口产品替代”的目标，取得了一次又一次的突破，积累了良好的客户口碑，得到了越来越多客户的肯定和支持！我们茂丰人还会继续前行，不改初心，为光机事业贡献我们的力量！

## 主要产品

Main Products

### 光学元器件

透镜、滤光片、棱镜、激光反射镜、偏振元件等



### 光学平台



### 电动精密定位台



### 手动精密定位平台



### 光学镜架



### 光学机械



### 光纤调整台



### 光学系统

(教学实验系统、LED量测系统、光通量测试系统等)、激光器和光学相关产品，也根据客户的需要设计和组装相关系统。



## 我们的优势

Our Advantages

- 1、我司已经通过了【GB/T19001-2016/ISO9001:2015质量管理体系认证】、【GB/T24001-2016/ISO14001:2015环境管理体系认证】和【高新技术企业认证】；
- 2、我司通过这么多年的技术积累，已经拥有多项专利技术，同时依托于科研院所的实力支撑，为推进 科研产业化贡献我们的力量；
- 3、我司产品种类覆盖比较全面，常规品备有库存，为客户科研提速；同时我司产业链比较完善，可以保障量产产品的供应周期；
- 4、我司产品自主研发，有经验丰富的工程师，可以快速响应客户的定制化需求，满足客户的个性化要求。

### 西格玛光机

OptoSigma



代理日本西格玛全系列的产品

MFOPT<sup>®</sup> 北京茂丰光电科技有限公司  
茂丰智光<sup>®</sup> Beijing Exuberance Opto-electronics Technology Co.,Ltd

打 / 造 / 中 / 高 / 端 / 光 / 电 / 实 / 验 / 室 / 器 / 材 / 品 / 牌

快 / 速 / 提 / 供 / 完 / 美 / 光 / 学 / 系 / 统 / 解 / 决 / 方 / 案

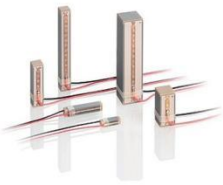
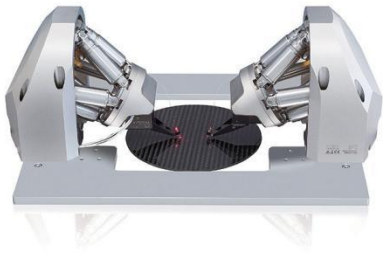
北京总部地址：北京市通州区赵登禹大街富力运河十号B02-2021  
华南办事处：广州市番禺区南村镇万博二路粤海广场830  
华东办事处：安徽省合肥市瑶海区王岗路龙湖瑶海天街2-607  
咨询电话：86-10-82600067 82601815 82601072

网站：www.mfopt.com 阿里巴巴国际站：mfopt.en.alibaba.com  
淘宝：mfopt.taobao.com 京东：mfopt.jd.com



迈微信光电

Micsense Photonics Instruments



PI

Physik Instrumente

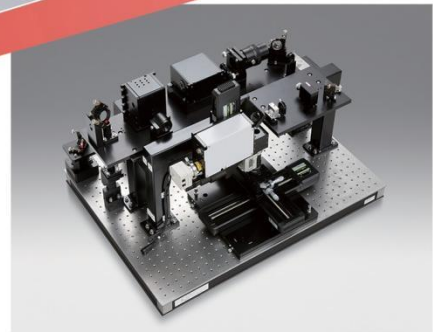
[微纳定位专家]

# Positioning Solutions

专业解决精密定位问题，从微米到亚纳米，从压电陶瓷到气浮轴承

- + 纳米台，气浮平台，电机平台，六足台，压电陶瓷电机/促动器
- + X,Y,Z,θX,θY,θZ 空间内全自由度定位产品
- + 负载范围0.1g至1000Kg，位移范围0.1nm至1000mm
- + 纳米级精度(重复精度1nm)，高速运动（3m/s），高频扫描（3KHz）

存志笃信 迈向精微



OptoSigma®

[光学解决方案]

# Laser Solution

西格玛光机是一个从研发到生产设备，都是用“光”解决问题的企业

Sigma Koki Group is your global supplier of quality solutions for broad range of applications from R&D to production equipment

## COMPONENTS



光学研磨产品 / 薄膜产品



镜架及 手动平台



自动应 用产品

从零件到组件 From Components to Units

## UNITS



干涉仪



电源



光学组件



运动控制

从组件到应用系统 From Units to Application System

## APPLICATION SYSTEM



激光加 工系统



调芯·焊接 系统

## ENVIRONMENT



环境·安全 产品

西安摘星光电科技有限公司(简称:摘星光电,STARTIN OPTRONICS)是光电领域的一家高科技公司。公司专注于为激光制造及应用行业提供科研与工业自动化解决方案。



我公司拥有“摘星光电”“STARTIN OPTRONICS”“钻研之友”“入微之目”“入化之目”等七个自主品牌。我公司在激光精密加工、激光飞时测距、激光脉冲雷达、激光光谱分析、激光测量等应用行业具有丰富经验积累，可以为用户提供成熟稳定的高品质标准产品，亦可根据用户的具体需求为用户提供完备的系统集成解决方案。

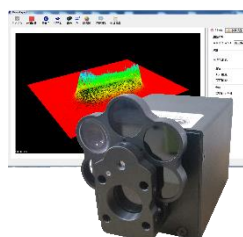
我公司激光系列产品涉及半导体激光封装模组，外腔半导体激光封装模组，固体微片激光模组，半导体激光器系统，窄线宽激光器系统，固体微片激光器系统，超快高能量脉冲固体激光器系统，MOPA 高能脉冲科研激光系统，OPO 可调谐激光系统，大功率/高能光纤激光器系统等激光部件及激光器系统产品。

我公司激光测量仪器系列产品包括激光功率与能量、光束质量与横模分析、激光光谱与纵模分析、激光脉冲与重频测量、激光偏振分析测量、波前与相位检测以及激光参数综合测量系统等激光测量仪器与系统检测解决方案。

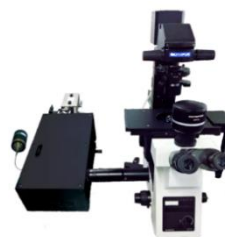
目前，我公司已经与国内 30 个省的 300 多家单位取得了长期密切地合作，其中包含国内众多知名高校、研究所、大型国企和高科技民营企业。



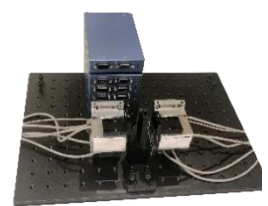
激光高精度制造技术



激光测量系统



材料科学与生命科学研究



微纳运动控制方案

企业官网: [www.startin-optronics.com](http://www.startin-optronics.com)

联系电话: 029-86521344

企业邮箱: [info@startin-optronics.com](mailto:info@startin-optronics.com)





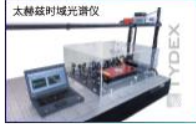
# 产品简介

PRODUCT INTRODUCTION

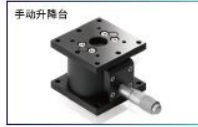


霍克光仪（北京）科技有限公司  
www.hawk-optics.cn admin@hawk-optics.com 8610-87578121

## ■ 太赫兹产品



## ■ 手动位移台



## 国外部分合作厂商



欢迎扫描下方二维码，关注微信公众号，可得到最新的产品信息，并参与积分抽奖活动。



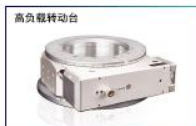
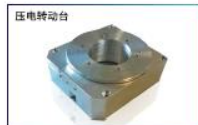
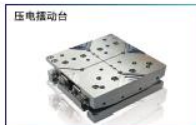
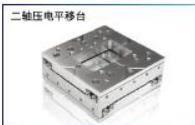
霍克光仪（北京）科技有限公司  
电话：(8610) 87578121  
传真：(8610) 82447165-8008  
邮件：admin@hawk-optics.com  
公司网站：http://www.hawk-optics.cn

## 公司简介 / COMPANY PROFILE

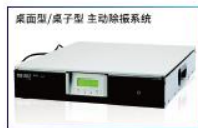
霍克光仪（北京）科技有限公司是一家从事光电产品设计及销售的高科技企业，主要致力于为客户提供专业的全套解决方案以及引进国外先进的技术和光电产品。产品种类涉及光学器件和精密微动机械、激光器、光谱仪及成像设备、光电子测试仪器、半导体检测设备百余品种，产品广泛应用于光谱研究、光纤通讯、航空航天、品质检测、国防军工、激光加工、LED检测、生物医疗及信息安全等相关领域，为科研和生产提供了一流的产品和专业的技术服务。

## 产品分类

### ■ 电动位移台



### ■ 隔振平台



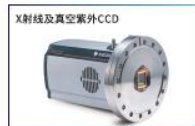
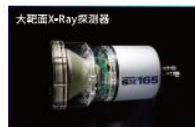
### ■ 光学支撑件及调整架



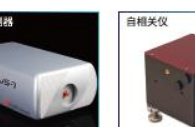
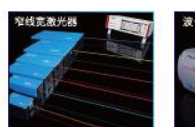
### ■ 光学镜片



### ■ 成像探测设备



### ■ 激光器及测量设备



# LBTEK

## 5000+ 产品, 极致购物体验

光学元件 · 光机械件 · 仪器设备 · 光学系统

专属顾问



价期透明



顺丰特快

新人礼包



全场包邮



当日发货



[www.lbtek.com](http://www.lbtek.com) | 🔍